

## The Isheyev meteorite: Mineralogy, petrology, bulk chemistry, oxygen, nitrogen, carbon isotopic compositions, and $^{40}\text{Ar}$ - $^{39}\text{Ar}$ ages

Marina A. IVANOVA<sup>1\*</sup>, Natalia N. KONONKOVA<sup>1</sup>, Alexander N. KROT<sup>2</sup>, Richard C. GREENWOOD<sup>3</sup>, Ian A. FRANCHI<sup>3</sup>, Alexander B. VERCHOVSKY<sup>3</sup>, Mario TRIELOFF<sup>4</sup>, Ekaterina V. KOROCHANTSEVA<sup>1,4</sup>, and Franz BRANDSTÄTTER<sup>5</sup>

<sup>1</sup>\*Vernadsky Institute of Geochemistry and Analytical Chemistry, Moscow 119991, Russia

<sup>2</sup>School of Ocean, Earth Science and Technology, Hawai'i Institute of Geophysics and Planetology, University of Hawai'i at Manoa, Honolulu, Hawaii 96822, USA

<sup>3</sup>Planetary and Space Sciences Research Institute, Open University, Milton Keynes, MK7 6AA, UK

<sup>4</sup>Mineralogisches Institut, Ruprecht-Karls-Universität Heidelberg, D-69120, Germany

<sup>5</sup>Natural History Museum, Vienna 1010, Austria

\*Corresponding author. E-mail: [venus2@online.ru](mailto:venus2@online.ru)

(Received 30 April 2007; revision accepted 30 September 2007)

**Abstract**—Isheyev is a metal-rich carbonaceous chondrite that contains several lithologies with different abundances of Fe,Ni metal (7–90 vol%). The metal-rich lithologies with 50–60 vol% of Fe,Ni metal are dominant. The metal-rich and metal-poor lithologies are most similar to the CB<sub>b</sub> and CH carbonaceous chondrites, respectively, providing a potential link between these chondrite groups. All lithologies experienced shock metamorphism of shock stage S4. All consist of similar components—Fe,Ni metal, chondrules, refractory inclusions (Ca, Al-rich inclusions [CAIs] and amoeboid olivine aggregates [AOAs]), and heavily hydrated lithic clasts—but show differences in their modal abundances, chondrule sizes, and proportions of porphyritic versus non-porphyritic chondrules. Bulk chemical and oxygen isotopic compositions are in the range of CH and CB chondrites. Bulk nitrogen isotopic composition is highly enriched in  $^{15}\text{N}$  ( $\delta^{15}\text{N} = 1122\text{\textperthousand}$ ). The magnetic fraction is very similar to the bulk sample in terms of both nitrogen release pattern and isotopic profile; the non-magnetic fraction contains significantly less heavy N. Carbon released at high temperatures shows a relatively heavy isotope signature. Similarly to CB<sub>b</sub> chondrites, ~20% of Fe,Ni-metal grains in Isheyev are chemically zoned. Similarly to CH chondrites, some metal grains are Ni-rich (>20 wt% Ni). In contrast to CB<sub>b</sub> and CH chondrites, most metal grains are thermally decomposed into Ni-rich and Ni-poor phases. Similar to CH chondrites, chondrules have porphyritic and non-porphyritic textures and ferromagnesian (type I and II), silica-rich, and aluminum-rich bulk compositions. Some of the layered ferromagnesian chondrules are surrounded by ferrous olivine or phyllosilicate rims. Phyllosilicates in chondrule rims are compositionally distinct from those in the hydrated lithic clasts. Similarly to CH chondrites, CAIs are dominated by the hibonite-, grossite-, and melilite-rich types; AOAs are very rare. We infer that Isheyev is a complex mixture of materials formed by different processes and under different physico-chemical conditions. Chondrules and refractory inclusions of two populations, metal grains, and heavily hydrated clasts accreted together into the Isheyev parent asteroid in a region of the protoplanetary disk depleted in fine-grained dust. Such a scenario is consistent with the presence of solar wind-implanted noble gases in Isheyev and with its comparatively old K-Ar age. We cannot exclude that the K-Ar system was affected by a later collisional event. The cosmic-ray exposure (CRE) age of Isheyev determined by cosmogenic  $^{38}\text{Ar}$  is ~34 Ma, similar to that of the Bencubbin (CB<sub>a</sub>) meteorite.

### INTRODUCTION

The CR (Renazzo-like), CH (metal-rich), and CB (Bencubbin-like) carbonaceous chondrites belong to a CR

chondrite clan (Weisberg et al. 1995; Krot et al. 2002a). All members of the clan are of petrologic types 2 and 3 and are among the most primitive materials formed in the early solar system, and, hence, can be potentially important for

understanding the evolution of the solar nebula (e.g., Weisberg et al. 2001; Krot et al. 2002a).

The CH chondrites are characterized by 1) the high abundance (~20 vol%) of Fe,Ni metal with an approximately solar Co/Ni ratio; some metal grains are chemically zoned or very Ni-rich (>20–30 wt%); 2) the small chondrule sizes (average diameter ~20  $\mu\text{m}$ ) with cryptocrystalline (CC) chondrules being dominant; the presence of porphyritic chondrules (type I and type II) and ferromagnesian, silica-rich, and Al-rich chemical types; 3) the presence of very refractory inclusions with grossite-rich and hibonite-rich CAIs being the dominant types; 4) the presence of Cr-rich troilite; 5) the bulk chemical compositions enriched in siderophile elements and depleted in moderately volatile elements with the degree of depletion positively correlated with volatility; 6) the bulk oxygen isotopic compositions plotting along the CR-mixing line; 7) the large positive anomalies of  $\delta^{15}\text{N}$  in bulk samples; 8) the presence of heavily hydrated CI-like lithic clasts (Greshake et al. 2002; Krot et al. 2002a), and 9) the general absence of fine-grained matrix materials between metal grains, chondrules, and refractory inclusions.

The CB chondrites are currently divided into the CB<sub>a</sub> (Bencubbin, Gujba, and Weatherford) and CB<sub>b</sub> (Hammadah al Hamra [HaH] 237, Queen Alexandra Range [QUE] 94411 paired with QUE 94627, and MacAlpine Hills [MAC] 02675) subgroups (Weisberg et al. 2001; Krot et al. 2005, 2006a). The CB<sub>a</sub> chondrites consist of 0.5–1 cm-sized compositionally uniform Fe,Ni metal  $\pm$  sulfide nodules (40–60 vol%), magnesian chondrules, and heavily hydrated lithic clasts. The chondrules are often fragmented and have skeletal/barred olivine-pyroxene textures; refractory inclusions are virtually absent (Weisberg et al. 2001; Krot et al. 2006a). The CB<sub>b</sub> chondrites consist of Fe,Ni metal (~70 vol%) and magnesian cryptocrystalline and skeletal/barred olivine-pyroxene chondrules (Krot et al. 2001a, 2002a, 2006a). Most metal grains are irregularly shaped and sulfide-free grains with a solar Co/Ni ratio; ~20% of them are chemically zoned; large, rounded compositionally uniform Fe,Ni metal  $\pm$  sulfide nodules are relatively rare. Very Ni-rich (>20–30 wt%) metal grains are absent. CAIs are rare and dominated by melilite, Al-diopside, and spinel; they have compact igneous textures and are typically surrounded by forsterite rims (Krot et al. 2001b). Like CH chondrites, the CB<sub>a</sub> and CB<sub>b</sub> chondrites are highly enriched in refractory and normal siderophile elements and depleted in moderately volatile and volatile elements, have bulk oxygen isotopic compositions plotting along the CR-mixing line (Clayton and Mayeda 1999) and  $^{15}\text{N}$ -enriched bulk nitrogen isotopic compositions.

To explain the anomalous characteristics of the CH and CB chondrites, both nebular and asteroidal models have been proposed (e.g., Grossman et al. 1988; Scott 1988; Weisberg et al. 1988; Wasson and Kallemeyn 1990; Bischoff et al. 1993a, 1993b; Meibom et al. 1999, 2000, 2001; Campbell et al. 2001, 2002; Petaev et al. 2001; Rubin et al. 2003;

Campbell and Humayun 2004; Weisberg et al. 2004; Krot et al. 2001a, 2001b, 2002a, 2005). Wasson and Kallemeyn (1990) concluded that Allan Hills (ALHA) 85085 is a “subchondritic” meteorite containing chondrules and metal grains produced during a highly energetic asteroidal collision mixed with typical (nebular) chondritic components. However, based on the elemental patterns of zoned metal showing volatility controlled behavior (Meibom et al. 1999, 2000) and  $^{16}\text{O}$ -enriched isotopic compositions of some chondrules and most of the refractory inclusions, it has been subsequently concluded that refractory inclusions, chondrules, and zoned metal grains in CH chondrites are in fact very pristine nebular products (e.g., Krot et al. 2002a). Based on the young absolute ages of Gujba and HaH 237, and mineralogical observations, indicating single-stage origin of chondrules and metal grains in these meteorites, Krot et al. (2005) concluded that the CB<sub>a</sub> and CB<sub>b</sub> chondrites are genetically related rocks. Chondrules and metal grains in both CB subgroups formed from a vapor-melt plume produced by a giant impact between planetary embryos after dust in the planetary disk had largely dissipated, supporting the earlier suggestions of Rubin et al. (2003) and Campbell and Humayun (2004). However, based on the magnesium isotopic compositions of chondrules and CAIs from the CB<sub>b</sub> chondrites and observations that some circumstellar disks around protostars last up to 10 Myr, Gounelle et al. (2007) concluded that the young absolute ages of CB chondrites are not inconsistent with their late nebular origin.

The recently discovered metal-rich meteorite Isheyev contains several lithologies, which have mineralogical characteristics intermediate between CH and CB<sub>b</sub> chondrites (Ivanova et al. 2006). Here we report the petrography, mineralogy, bulk chemistry, oxygen, nitrogen, and, carbon isotopic compositions,  $^{40}\text{Ar}$ – $^{39}\text{Ar}$  and cosmic exposure ages of Isheyev, and discuss possible origin of this meteorite and possible implication for understanding genetic relationships between the CH and CB chondrites. The detailed mineralogy and petrography of chondrules and refractory inclusions from Isheyev are described in detail by Krot et al. (2007b, 2007c).

## SAMPLES AND ANALYTICAL PROCEDURES

Fourteen polished sections of Isheyev with a total surface area of ~30  $\text{cm}^2$  were studied by optical microscopy, backscattered electron (BSE) imaging, and electron probe microanalysis at Vernadsky Institute, University of Vienna, and University of Hawai'i. All sections were mapped in Ca, Al, Mg, Ni, and Si K $\alpha$  X-rays using fully focused electron beam, 15 kV accelerating voltage, 30–100 nA beam current, 20–30 ms per pixel acquisition time, and resolution of ~2–3  $\mu\text{m}$  per pixel with a Cameca SX-100 electron microprobe at Vernadsky Institute and Cameca SX-50 at University of Hawai'i. The elemental maps in Mg, Ca, and Al K $\alpha$  were combined using a RGB-color scheme (Mg-red, Ca-green, Al-blue) and ENVI (Environment for Visualizing Images)

software package. The identified chondritic components were studied in backscattered electrons (BSE) with the JEOL JSM-6400 and JEOL 5900LV scanning electron microscopes (SEM) equipped with energy dispersive spectrometers (EDS). Mineral compositions were determined with the Cameca SX-100 and SX-50 electron microprobes using 15 kV accelerating voltage and fully focused beam with currents of 20 nA for silicates and 30 nA for metals. Well-characterized silicates, oxides, metals, and sulfides were used as standards. Matrix corrections were applied using a PAP software routine.

Bulk compositions of chondrules and refractory inclusions were measured by acquiring  $\sim 15 \times 15 \mu\text{m}$  rastered beam analyses along profiles covering a whole object. Detection limits in silicates were  $\text{SiO}_2$ ,  $\text{TiO}_2$ ,  $\text{Al}_2\text{O}_3$ ,  $\text{Cr}_2\text{O}_3$ ,  $\text{FeO}$ ,  $\text{MnO}$ ,  $\text{MgO}$ ,  $\text{CaO}$ ,  $\text{NiO}$ —0.02 wt%;  $\text{K}_2\text{O}$ ,  $\text{Na}_2\text{O}$ —0.05 wt%.

A 10 g sample was crushed and powdered in an agate mortar in order to get a representative average sample for bulk-rock major and trace element determinations. Magnetic (88.43 wt%) and non-magnetic (11.57 wt%) fractions were prepared for analyses. 100 mg of each fraction were analyzed for Hf, Al, Sc, Lu, Tb, Ti, La, Ca, V, Sm, Nd, Ce, Yb, Eu, Mg, Cr, Mn, K, Na, Zn, Se, Ir, Ni, Co, Fe, Pd, Au, As, and Cu using inductively coupled plasma mass-spectrometry (ICP-MS). A 300 mg sample of the metal-rich lithology of Isheyev was used for measurements of Si, Ti, Al, Cr, Fe, Mn, Mg, Ca, Na, K, and S using X-ray fluorescence (XRF) analysis. A 20 mg chip of the metal-rich lithology of Isheyev was analyzed by instrumental neutron activation analyses (INAA) for La, Ce, Nd, Sm, Eu, Tb, Yb, Lu, Na, Ca, Sc, Cr, Fe, Co, Ni, Se, As, Hf, Au, Ir.  $\text{H}_2\text{O}$  and S were measured with a CHN analyzer from both magnetic and non-magnetic fractions. We used a combination of all methods for characterization of Isheyev bulk composition represented in Table 4. Bulk composition of a 1 g sample of the CH chondrite Northwest Africa (NWA) 470 analyzed by ICP-MS, XRF, and CHN analyzer are listed in Table 4 as well.

A separate split of the metal-rich lithology, weighing  $\sim 50$  mg, was used to measure bulk oxygen, nitrogen, and carbon isotopic compositions at the Open University. The sample was crushed in an agate mortar and pestle. Oxygen isotopic compositions were determined in replicate on  $\sim 2$  mg aliquots of the partly homogenized sample by laser fluorination. The samples were heated with a  $\text{CO}_2$  laser ( $10.6 \mu\text{m}$ ) in the presence of excess  $\text{BrF}_5$ , the gas purified over hot  $\text{KBr}$  and cryogenic traps and then analyzed on a PRISM III mass spectrometer (VG Isogas Ltd.). Analytical precision is  $\sim \pm 0.8\%$  and  $\pm 1.6\%$  ( $2\sigma$ ) for  $\delta^{17}\text{O}$  and  $\delta^{18}\text{O}$ , respectively, providing a precision of  $\sim \pm 1.7\%$  ( $2\sigma$ ) for  $\Delta^{17}\text{O}$ . Details of the procedure are described by Miller et al. (1999).

Nitrogen and carbon isotopic compositions were determined simultaneously using the Finesse machine, a complex of three static mode mass-spectrometers fed from a single extraction system (Wright et al. 1988; Wright and Pillinger 1989; Verchovsky et al. 1998). The analytical

precision is  $\sim \pm 1\%$  for both  $\delta^{13}\text{C}$  and  $\delta^{15}\text{N}$  measurements. Nitrogen and carbon were extracted by stepped combustion in the temperature range from 200 to 1400 °C. Additional magnetic and a non-magnetic fraction were analyzed for carbon and nitrogen by stepped combustion.

The  ${}^{40}\text{Ar}$ - ${}^{39}\text{Ar}$  study was performed using a metal-rich whole rock sample weighing  $\sim 72$  mg. The analytical procedure of  ${}^{40}\text{Ar}$ - ${}^{39}\text{Ar}$  analysis is described by Jessberger et al. (1980) and Trieloff et al. (1998, 2003a, 2003b, 2005). Samples were irradiated for 20 days, using high-purity Al foil and Cd shielding at the GKSS-reactor in Geesthacht, Germany. The  $J$  value was  $0.86 \times 10^{-2}$  as determined by NL25 hornblende flux monitors (Schäffer and Schäffer 1977). Correction factors for interfering isotopes determined by  $\text{CaF}_2$  monitors were  $({}^{36}\text{Ar}/{}^{37}\text{Ar})_{\text{Ca}} = (4.3 \pm 0.2) \times 10^{-4}$ ,  $({}^{38}\text{Ar}/{}^{37}\text{Ar})_{\text{Ca}} = (8.8 \pm 0.2) \times 10^{-5}$ ,  $({}^{39}\text{Ar}/{}^{37}\text{Ar})_{\text{Ca}} = (9.8 \pm 0.1) \times 10^{-4}$ ,  $({}^{38}\text{Ar}/{}^{39}\text{Ar})_{\text{K}} = (1.79 \pm 0.08) \times 10^{-2}$  was determined via the NL25 monitors, after subtraction of Cl-induced  ${}^{38}\text{Ar}$ .  $({}^{40}\text{Ar}/{}^{37}\text{Ar})_{\text{Ca}} = (3 \pm 3) \times 10^{-3}$  were determined by Turner (1971) and  $({}^{40}\text{Ar}/{}^{39}\text{Ar})_{\text{K}} = (1.23 \pm 0.24) \times 10^{-2}$  by Brereton (1970). The samples were stepwise heated to temperatures from 400 °C to 1460 °C (16 temperature steps) using a resistance-heated furnace with  ${}^{40}\text{Ar}$  blank values of  $4 \times 10^{-10}$  ccSTP at 800 °C and  $15 \times 10^{-10}$  ccSTP at 1400 °C (20 min heating duration). Apparent ages were calculated using the Steiger and Jäger (1977) conventions.

The cosmic-ray exposure (CRE) age was calculated from the total amount of cosmogenic  ${}^{38}\text{Ar}$ . The production rate was determined by the method of Eugster (1988) using the measured bulk-rock chemical composition of Isheyev. The  ${}^{38}\text{Ar}$  production rate was lowered by 13% as recommended by Schultz et al. (1991).

## RESULTS

### Lithologies

Petrographic observations of 14 sections of Isheyev indicate that the meteorite is mostly metal-rich and on average contains  $\sim 60$  vol% of Fe,Ni metal. However, several sections contain multiple lithologies with different contents of Fe,Ni metal—between 90 and 7 vol% (Figs. 1 and 2; see also Fig. 1 in Krot et al. 2006b, 2006c). Lithologies with the highest and the lowest abundances of Fe,Ni metal are rare. Section shown in Fig. 1 has four lithologies, #1, #2, #3, and #4, with 7, 20, 52, and 60 vol% of Fe,Ni metal, respectively. The boundaries between the lithologies are either sharp (Fig. 1) or gradational (Fig. 2). For example, one boundary between lithology #1 and lithology #4 is distinct, being defined by a sharp change of metal/silicate ratio across the boundary (Fig. 1); in another part of this section, however, the boundary between these lithologies is gradational. As a result, in some cases, it is difficult to recognize a boundary between the lithologies.

All lithologies in Isheyev have similar sets of chondritic

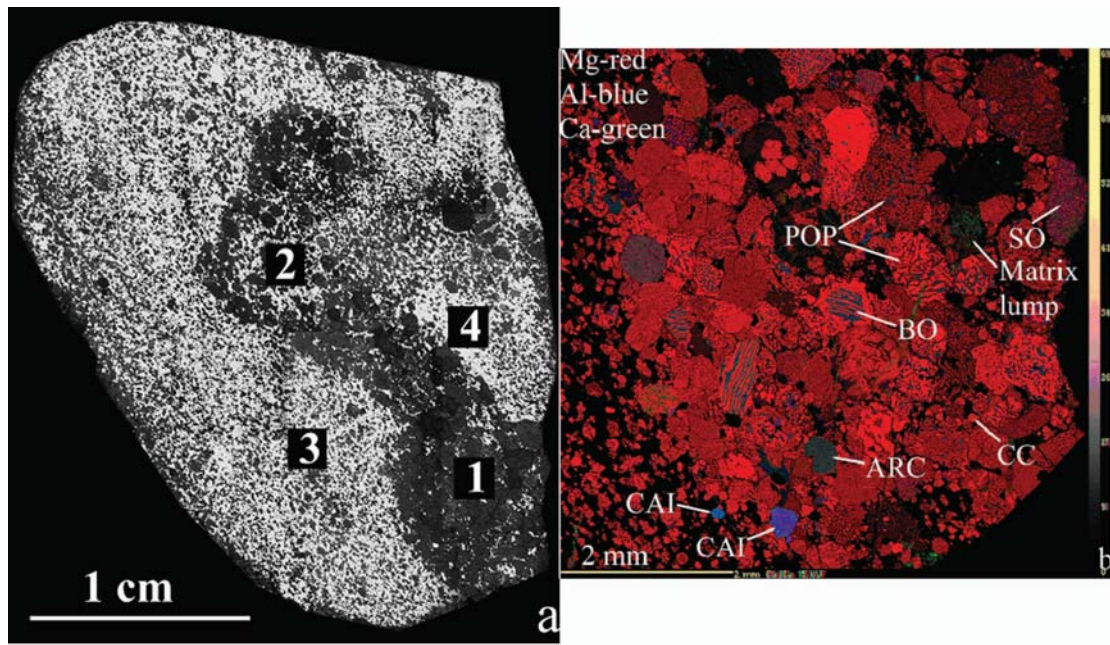


Fig. 1. Optical micrograph in reflected light (a) and combined elemental map in Mg (red), Ca (green), and Al K $\alpha$  (blue) X-rays (b) of the metal-poor lithology #1 and two metal-rich lithologies, #3 and #4, of Isheyev. There are sharp and gradational contacts between the lithologies composed of the similar components (chondrules, refractory inclusions, Fe,Ni metal, and hydrated lithic clasts), which, however, have different sizes. In addition, the metal-poor lithology contains higher abundance of porphyritic chondrules. ARC = Al-rich chondrule; BO = barred olivine; CAI = Ca,Al-rich inclusion; CC = cryptocrystalline; POP = porphyritic olivine-pyroxene; SO = skeletal olivine.

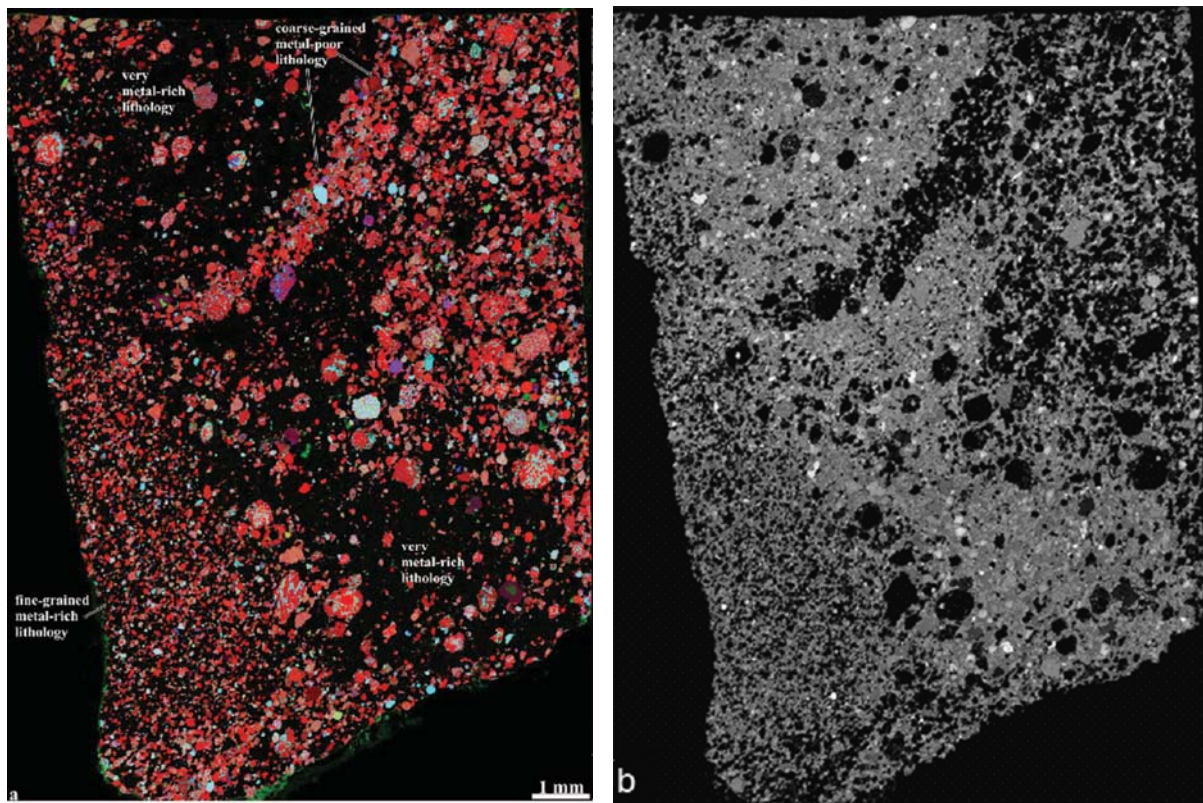


Fig. 2. Combined elemental map in Mg (red), Ca (green), and Al K $\alpha$  (blue) X-rays (a) and elemental maps in Ni K $\alpha$  (b) of Isheyev. This section contains three lithologies with different grain sizes, metal/chondrule ratios, and porphyritic versus non-porphyritic chondrules. The boundaries between the lithologies are gradational.

Table 1. Proportions (%) of different textural types of chondrules and chondrule sizes (mm) from the metal-poor and the metal-rich lithologies.

	Porphyritic	Skeletal	Cryptocrystalline	Barred	Chondrule sizes
Metal-poor lithology (#1, 2)	53	30	9	7	0.1–1
Metal-rich lithology (#3, 4)	29	54	14	1.4	0.02–0.4

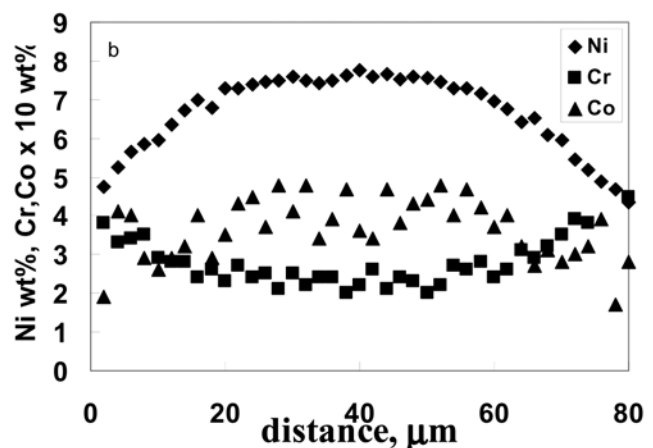
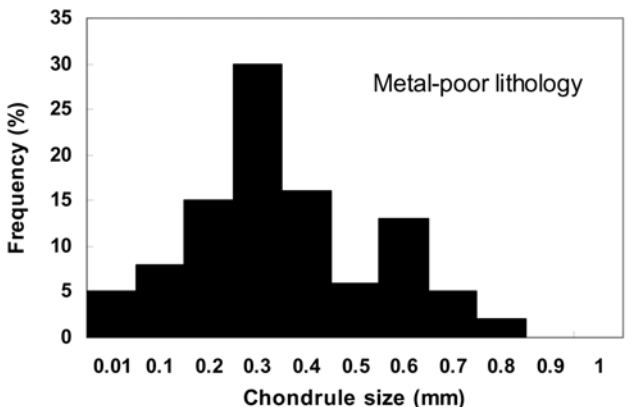
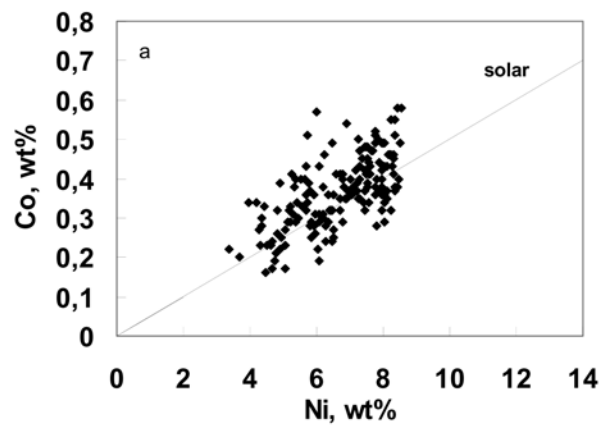
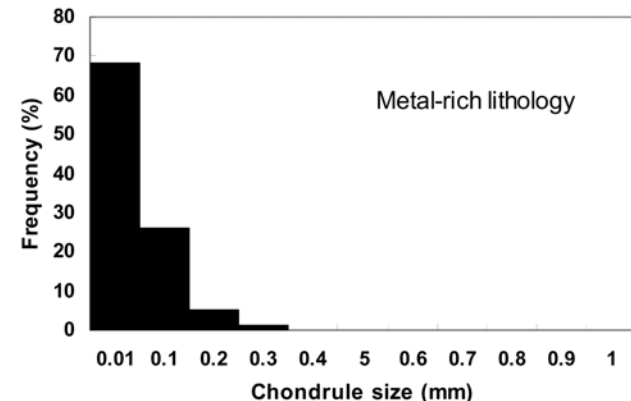


Fig. 3. Chondrule size distributions in the metal-poor (#1 and #2) and metal-rich (#3 and #4) lithologies of Isheyev. The metal-rich lithology contains smaller chondrules (0.1–0.4 mm) than the metal-poor lithologies (0.2–1 mm).

components and consist of Fe,Ni metal, chondrules, heavily hydrated lithic clasts, and rare CAIs and AOAs; no fine-grained matrix-like material is observed between these coarse components. Occasionally, thin layers of shock melts occur between the coarse-grained components. All lithologies contain zoned Fe,Ni metal grains and unzoned Ni-rich (>25 wt% Ni) metal grains (Fig. 2b).

There are differences in textural types and sizes of chondrules between the lithologies. The metal-rich lithologies typically contain smaller chondrules (0.02–0.4 mm), 0.10 mm in average, than the metal-poor lithologies (0.1–1 mm), 0.40 mm in average (Fig. 3); metal grains have similar size range (0.1–0.3 mm) and average sizes, 0.22 and 0.24 mm, respectively. The metal-rich lithologies have higher proportions of chondrules with non-porphyritic (cryptocrystalline, barred, skeletal) textures versus

chondrules with porphyritic (olivine, olivine-pyroxene, and pyroxene) textures than those in the metal-poor lithologies (Table 1).

### Chondritic Components

#### Fe,Ni metal

The Isheyev meteorite contains chemically homogeneous and zoned Fe,Ni-metal grains (Figs. 4 and 5). The unzoned metal grains contain 4.2–14.3 wt% Ni, 0.2–0.5 wt% Co, and 0.03–0.6 wt% Cr; Ni and Co are positively correlated; the Co/Ni ratio is solar (Fig. 4a). Rare unzoned metal grains are rich in Ni (>25 wt%) and Co (0.6 wt%). Some of the Ni-poor homogeneous or slightly decomposed metal grains contain rounded inclusions of Cr-rich (2.5–

Table 2. Chemical compositions of different types of chondrules from Isheyev (in wt%).

	N	SiO <sub>2</sub>	TiO <sub>2</sub>	Al <sub>2</sub> O <sub>3</sub>	Cr <sub>2</sub> O <sub>3</sub>	FeO	MnO	MgO	CaO	Na <sub>2</sub> O	K <sub>2</sub> O	NiO	Total
POP. Type I	6	40.0–49.2	0.05–0.50	1.23–9.50	0.09–0.63	1.88–4.79	0.01–0.22	34.1–48.0	0.81–8.16	0.01–0.37	0.01–0.17	0.03–0.21	
		45.3	0.27	5.91	0.43	3.35	0.10	40.1	4.52	0.11	0.03	0.08	100.2
POP. Type II	4	37.1–55.3	0.03–0.24	1.43–8.93	0.16–2.63	12.7–34.7	0.21–0.78	8.30–39.8	1.03–2.69	0.32–3.13	0.01–0.58	0.02–0.23	
		44.1	0.13	3.45	0.74	23.0	0.46	24.0	2.33	1.51	0.19	0.11	100.0
CC. MgO-rich	4	49.5–56.1	0.01–0.06	0.22–1.20	0.77–0.81	0.48–2.50	0.06–0.13	42.3–44.0	0.16–1.01	<0.05	<0.05	<0.02	
		53.1	0.04	0.67	0.78	1.94	0.09	43.24	0.56	0.01			100.4
CC. FeO-rich	3	37.8–51.1	0.01–0.10	0.04–2.00	0.36–0.93	12.5–27.7	0.14–0.31	25.9–34.9	0.11–1.30	0.04–0.96	0.01–0.27	0.02–0.20	
		45.1	0.06	0.97	0.64	20.3	0.20	30.4	0.70	0.28	0.08	0.08	98.8
SO. MgO-rich	4	46.3–52.9	0.15–0.52	3.92–11.5	0.44–0.85	3.59–5.01	0.03–0.38	27.6–35.6	3.64–8.30	0.01–0.19	<0.05	<0.02	
		48.9	0.35	8.45	0.56	4.57	0.12	31.6	6.18	0.07			100.9
BO. MgO-rich	3	42.9–46.1	0.46–0.60	11.8–12.4	0.15–0.45	2.77–3.60	0.02–0.03	27.4–29.1	9.34–12.0	0.02–0.03	<0.05	0.02–0.05	
		44.5	0.53	12.1	0.3	3.18	0.03	28.2	10.7	0.03	0.01	0.04	99.6
BO. FeO-rich	2	32.1–42.5	0.11–0.21	1.62–5.07	0.43–0.73	23.0–39.6	0.20–0.37	23.4–40.4	0.47–1.99	0.38–0.62	0.01–0.18	0.02–0.10	
		38.5	0.13	2.79	0.66	26.2	0.26	29.7	1.58	0.47	0.05	0.08	100.3

N = number of chondrules; POP = porphyritic olivine; CC = cryptocrystalline; SO = skeletal olivine. BO = barred olivine.

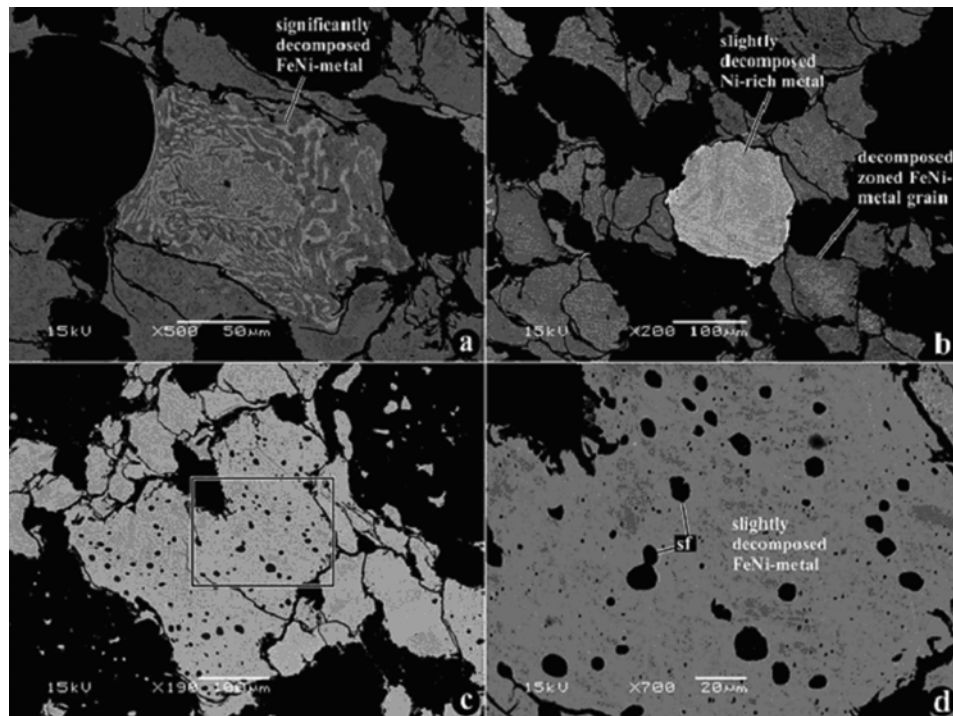


Fig. 5. BSE images of Fe,Ni-metal grains from Isheyev. About 20–30% of metal grains show concentric zoning with Ni and Co contents increasing towards the periphery. Most metal grains are decomposed into Ni-rich and Ni-poor phases (a, b). Rare metal grains are Ni-rich; some contain abundant inclusions of Cr-bearing sulfides (sf) (c, d).

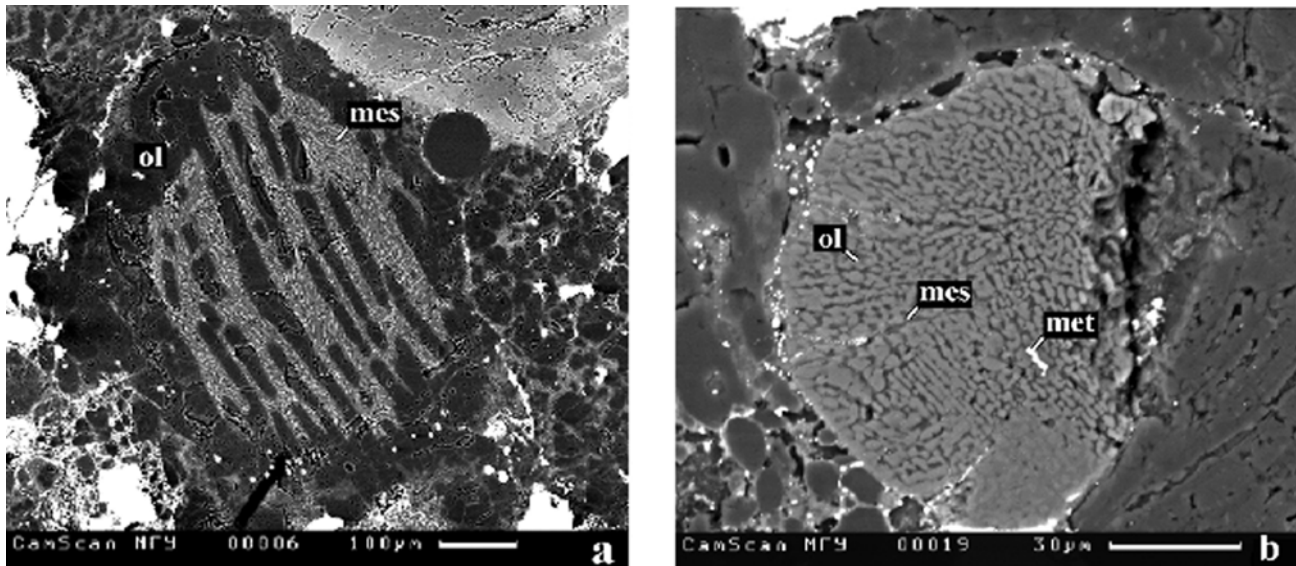


Fig. 6. BSE images of chondrules with barred (a) and skeletal olivine (b) textures. Chondrules of both textural types have magnesian (a) or ferrous (b) bulk compositions and occur in the metal-rich and metal-poor lithologies of Isheyev. ol = olivine; mes = glassy or microcrystalline mesostasis; met = FeNi-metal grains.

13 wt%) troilite (Fig. 5b). About 20–30% of Fe,Ni-metal grains in Isheyev are chemically zoned with Ni and Co decreasing and Cr increasing towards the edges of the grains (Fig. 4b). Most zoned grains show evidence for decomposition into Ni-rich and Ni-poor phases (Fig. 5a). These phases are generally too fine-grained to resolve using electron microprobe analysis.

#### Chondrules

The Isheyev chondrules have various textural types: cryptocrystalline (CC), barred olivine (BO), skeletal olivine ± pyroxene (SO), radial pyroxene (RP), porphyritic olivine (PO), porphyritic olivine-pyroxene (POP), and porphyritic pyroxene (PP), and show a range of bulk chemical compositions: ferromagnesian (type I and II), Al-rich

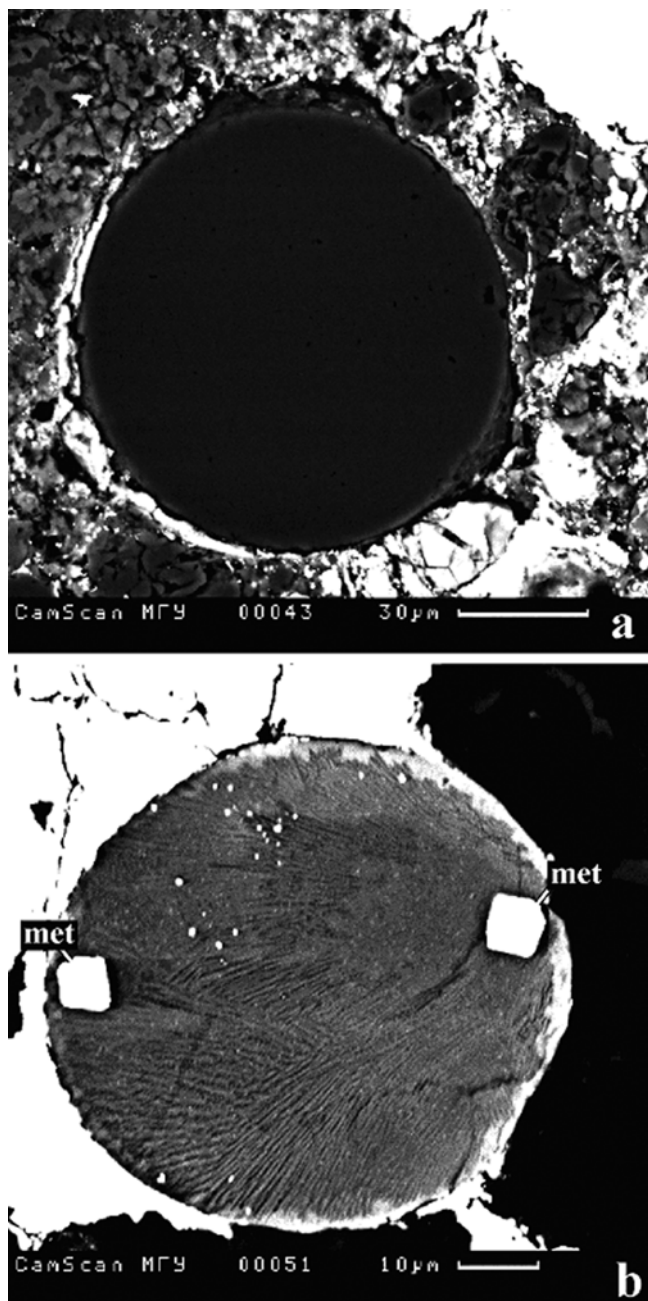


Fig. 7. BSE images of the magnesian cryptocrystalline chondrule (a) and radial pyroxene ferrous chondrule (b) textures from the metal-rich lithology of Isheyev. The latter contains euhedral Fe,Ni-metal (met) grains.

(>10 wt%  $\text{Al}_2\text{O}_3$ ; Bischoff and Keil 1984), and silica-rich (>65 wt%  $\text{SiO}_2$ ; Hezel et al. 2003). Both porphyritic and non-porphyritic chondrules can be ferromagnesian or Al-rich. For a detailed description of textures and mineralogy of the Isheyev chondrules, see Krot et al. (2006b).

BO chondrules consist of olivine bars and Ca-rich glassy mesostasis; some of the chondrules have continuous olivine shells (Figs. 6a–b). SO chondrules are texturally similar to

BO chondrules, but lack olivine shells and consist of olivine overgrown by low-Ca pyroxene and high-Ca pyroxene, and glassy or microcrystalline mesostasis (Figs. 6c–d); both pyroxenes contain high Al contents.

CC and RP chondrules have spheroidal shapes and magnesian and ferrous compositions (Figs. 7a–b). The magnesian CC chondrules are dominant; they have olivine-pyroxene-normative compositions and low  $\text{CaO}$ ,  $\text{Al}_2\text{O}_3$ ,  $\text{TiO}_2$ , and  $\text{MnO}$  contents (Table 2). Although magnesian CC chondrules are metal-free, some of them occur as inclusions inside chemically zoned Fe,Ni-metal grains (Fig. 7b in Krot et al. [2006b]). Ferrous RP chondrules contain higher  $\text{MnO}$  and  $\text{Na}_2\text{O}$  contents than magnesian CC chondrules and often show inverse compositional zoning with  $\text{FeO}$  contents decreasing towards the periphery. This zoning can be accompanied by tiny inclusions of metal in chondrule peripheries indicative of reduction. One of the ferrous fine-grained chondrules contains euhedral inclusions of Fe,Ni metal (Fig. 7b); similar chondrules have been previously described in CH chondrites (Krot et al. 2000).

Porphyritic chondrules can be divided into magnesian (type I), ferrous (type II), and Al-rich. Type I chondrules are dominant; they consist of forsteritic olivine ( $\text{Fa}_2$ ) and magnesium-rich low-Ca pyroxene ( $\text{Fs}_2\text{Wo}_{1-2}$ ) phenocrysts and glassy or fine-grained mesostasis (Fig. 8). Occasionally, low-Ca pyroxene forms a continuous shell around an olivine-rich core. Rare relict CAIs were reported in type I chondrules (Krot et al. 2006a, 2006b, 2007a), but coarse-grained igneous rims or independent compound chondrules were not observed. Some of the magnesian porphyritic chondrules are highly enriched in Fe,Ni-metal nodules.

Type II chondrules consist of zoned ferrous olivine ( $\text{Fa}_{10-38}$ ) and low-Ca pyroxene ( $\text{Fs}_{10-12}\text{Wo}_{1-2}$ ) phenocrysts, alkali-rich glassy or microcrystalline mesostasis, and minor chromite, troilite, and Ni-rich metal (Fig. 9). A few type II chondrules contain relict grains of magnesian olivine and low-Ca pyroxene; coarse-grained igneous rims or compound chondrules were not observed.

Aluminum-rich chondrules can be divided into Al-diopside-rich and plagioclase-rich (Fig. 10). The Al-diopside-rich chondrules consist of skeletal forsterite overgrown by Al-diopside,  $\pm$ spinel, and fine-grained, Ca,Al,Mg-rich mesostasis. Similar chondrules are commonly observed in CH and CB chondrites (Krot et al. 2001b). The plagioclase-rich chondrules consist of anorthitic plagioclase, forsteritic olivine, low-Ca pyroxene, high-Ca pyroxenes, Fe,Ni metal, and  $\pm$ spinel. Some of these chondrules contain relict refractory inclusions (see Krot et al. 2006b, 2006c). These chondrules are texturally and mineralogically similar to most of the Al-rich chondrules described in carbonaceous chondrites (e.g., Krot and Keil 2002; Krot et al. 2002b). Bulk chemical compositions of two Al-rich chondrules are presented in Table 3.

Silica-rich chondrules consist of low-Ca pyroxene, high-

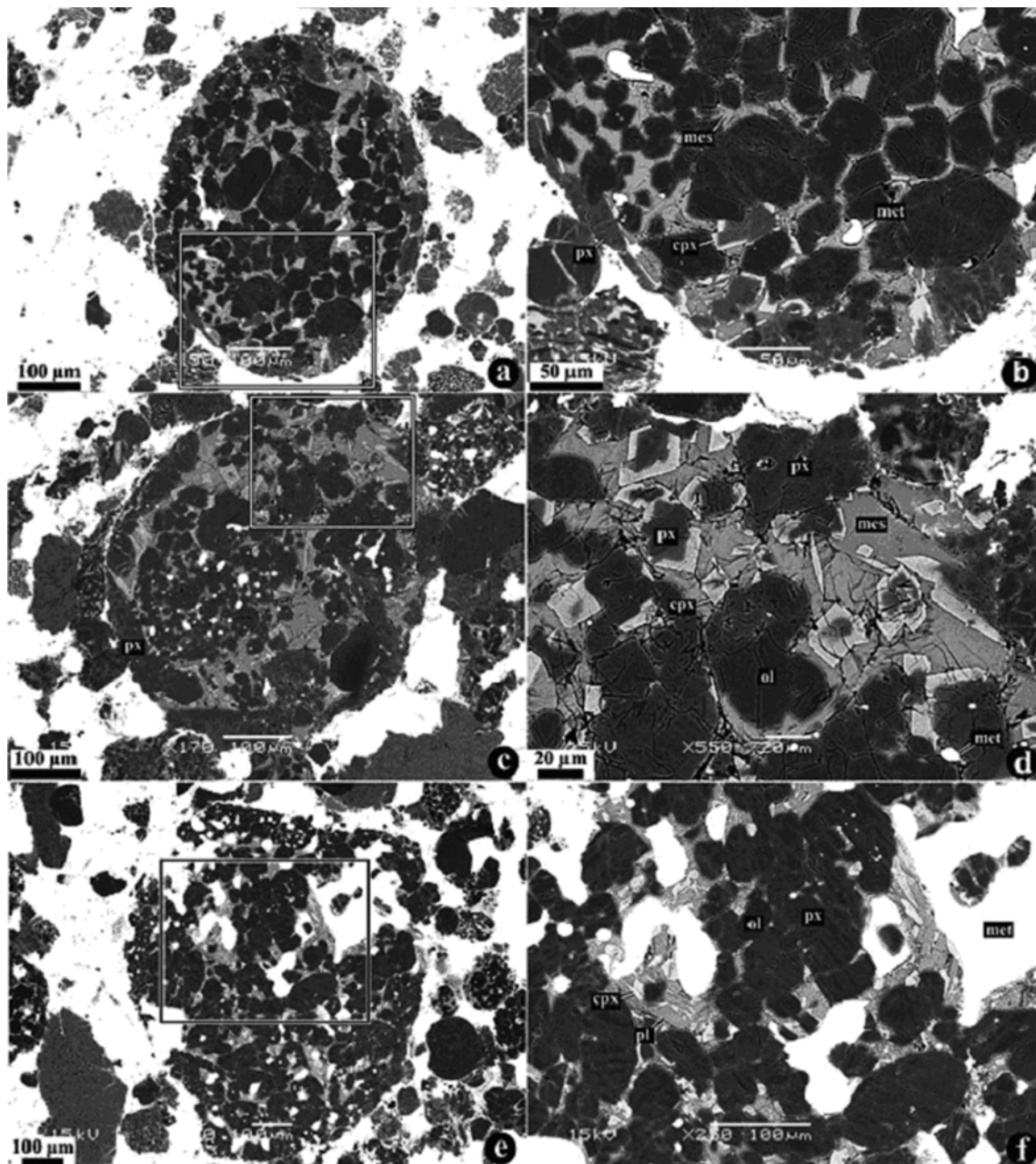


Fig. 8. BSE images of magnesian porphyritic olivine (a, b), porphyritic olivine-pyroxene (c, d), and porphyritic pyroxene (e, f) chondrules from Isheyev. Regions outlined in (a), (c), and (d) are shown in detail in (b), (e), and (f), respectively. cpx = high-Ca pyroxene; mes = mesostasis; met = Fe,Ni metal; ol = olivine; pl = plagioclase; px = low-Ca pyroxene.

Ca pyroxene, silica, and glassy mesostasis (Fig. 11). They have textures and compositions similar to those described by Hezel et al. (2003) in CH chondrites. Several chondrules composed of silica and ferromagnesian pyroxene are surrounded by a very fine-grained material, possible hydrated alteration minerals (Fig. 11a).

#### *Layered Chondrules*

Several chondrules, 40–90 µm in diameter, were found in the metal-rich lithology. They are mineralogically zoned and

have a magnesian core composed of low-Ca pyroxene ( $\text{Fs}_{1.6-23}$ ) or olivine ( $\text{Fa}_{14}$ ), that is surrounded by a rim (3–15 µm in size) of ferrous olivine ( $\text{Fa}_{60-72}$ ) or phyllosilicates (Table 3; Fig. 12). Some of the zoned chondrules have cryptocrystalline textures (Fig. 12a) and contain tiny inclusions of Fe,Ni metal. Similar layered chondrules have been previously described in the CH chondrites NWA 470 (Ivanova et al. 2001), ALHA85085 (Krot et al. 2000), and Acfer 182 (Hezel et al. 2002). No traces of reactions between phyllosilicate rims and surrounding materials were observed.

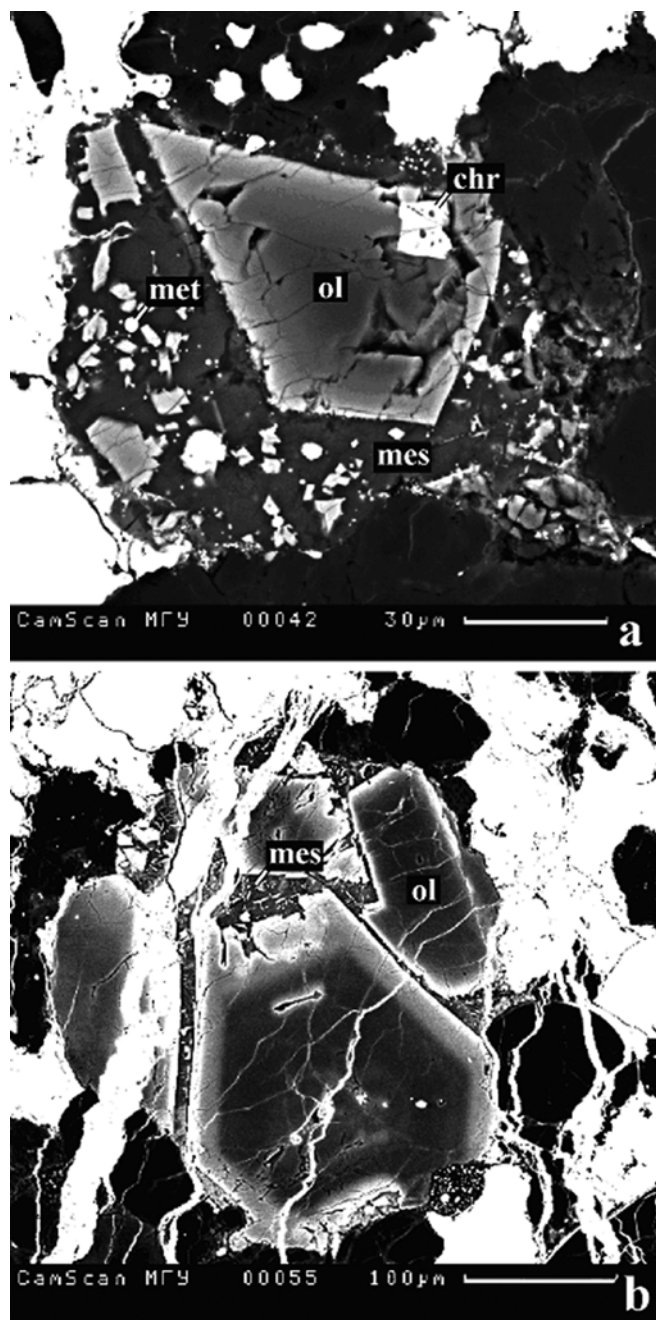


Fig. 9. BSE images of ferrous porphyritic olivine (type II) chondrules from Isheyev. The chondrules consist of ferrous olivine, low-Ca pyroxene, alkali-rich mesostasis, rare chromite, sulfides, and Ni-rich metal. mes = mesostasis; met = Ni-rich metal; ol = olivine; px = low-Ca pyroxene; chr = chromite. Relict cores are dark-grey in the crystals of olivine (b).

#### Refractory Inclusions

Refractory inclusions are found in all Isheyev lithologies (Krot et al., Forthcoming). The metal-rich lithologies contain a higher abundance of refractory inclusions than the metal-poor lithologies. About 60% of the Isheyev CAIs are compact, rounded or ellipsoidal objects,

40–190  $\mu\text{m}$  in size, which probably crystallized from melts. Based on the major mineralogy, these refractory spherules can be divided into hibonite-pyroxene-rich (Figs. 13a–b), grossite-rich (Fig. 13c), melilite-rich, and spinel-rich. They have either no rims around them or are surrounded by thin layers of melilite and/or Al-diopside; secondary anorthite replacing melilite is virtually absent. The other 40% of CAIs are less refractory, rounded or irregularly shaped objects composed of melilite, spinel, Al,Ti-diopside, and anorthite; most of them are surrounded by the Wark-Lovering rims of spinel  $\pm$  hibonite, melilite, Al-diopside, and  $\pm$ forsterite (Figs. 13d–f). These CAIs often contain secondary anorthite replacing melilite. Some of the anorthite-diopside-rich CAIs are igneous objects and can be classified as Type C inclusions (Krot et al., Forthcoming). In addition, there are rare isolated spinel grains, which could have resulted from fragmentation of the Al-diopside-spinel-rich inclusions. Bulk compositions of representative CAIs are listed in Table 4.

AOAs are exceptionally rare in Isheyev. They consist of forsteritic olivine, anorthite, Al-diopside, Fe,Ni metal, and minor spinel. Neither CAIs nor AOAs show evidence for Fe-alkali metasomatic or aqueous alteration.

#### Heavily Hydrated Lithic Clasts

Heavily hydrated lithic clasts consist of phyllosilicates, lath-shaped Fe,Ni-sulfides, Ca- and Mg-rich carbonates, and magnetite; the latter has platy and framboidal morphologies (Fig. 14). Phyllosilicates in the clasts are less Fe-rich than those in rims around zoned chondrules (Fig. 15). Similar clasts have been previously described in CH chondrites and the CB<sub>b</sub> chondrite QUE 94411 (Greshake et al. 2002).

#### Bulk Chemical Compositions

Bulk chemical composition of Isheyev is listed in Table 4 and shown in Figs. 16a–b. The Mg-and CI-normalized refractory lithophile abundance pattern of the Isheyev whole rock is enriched by a factor of  $\sim 1.3$ . This is a mean value for refractory lithophiles with condensation temperature above Mg. Similar enrichments were reported for the CB<sub>b</sub> chondrites HaH 237 ( $1.3 \times \text{CI}$ ) (Zipfel et al. 1998) and QUE 94411 ( $1.5 \times \text{CI}$ ) (Weisberg et al. 2001) and the CH chondrite NWA 470 (Table 5). The CH chondrites, ALHA85085 and Acfer 182, are characterized by approximately solar abundances of refractory lithophile elements. La content is higher than other elements ( $1.8 \times \text{CI}$ ); it is similar to that of QUE 94411. The Mg-normalized abundances of Na and K are highly depleted ( $0.09$  and  $0.14 \times \text{CI}$ , respectively). Interestingly, the concentration of the moderate volatile element Cr is high ( $1.58 \times \text{CI}$ ); even higher Cr enrichment was reported for QUE 94411 ( $2.33 \times \text{CI}$ ) and HaH 237 ( $2.4 \times \text{CI}$ ; Zipfel et al. 1998). The Mg- and CI-normalized siderophile element abundance patterns for elements with condensation temperatures above condensation temperature

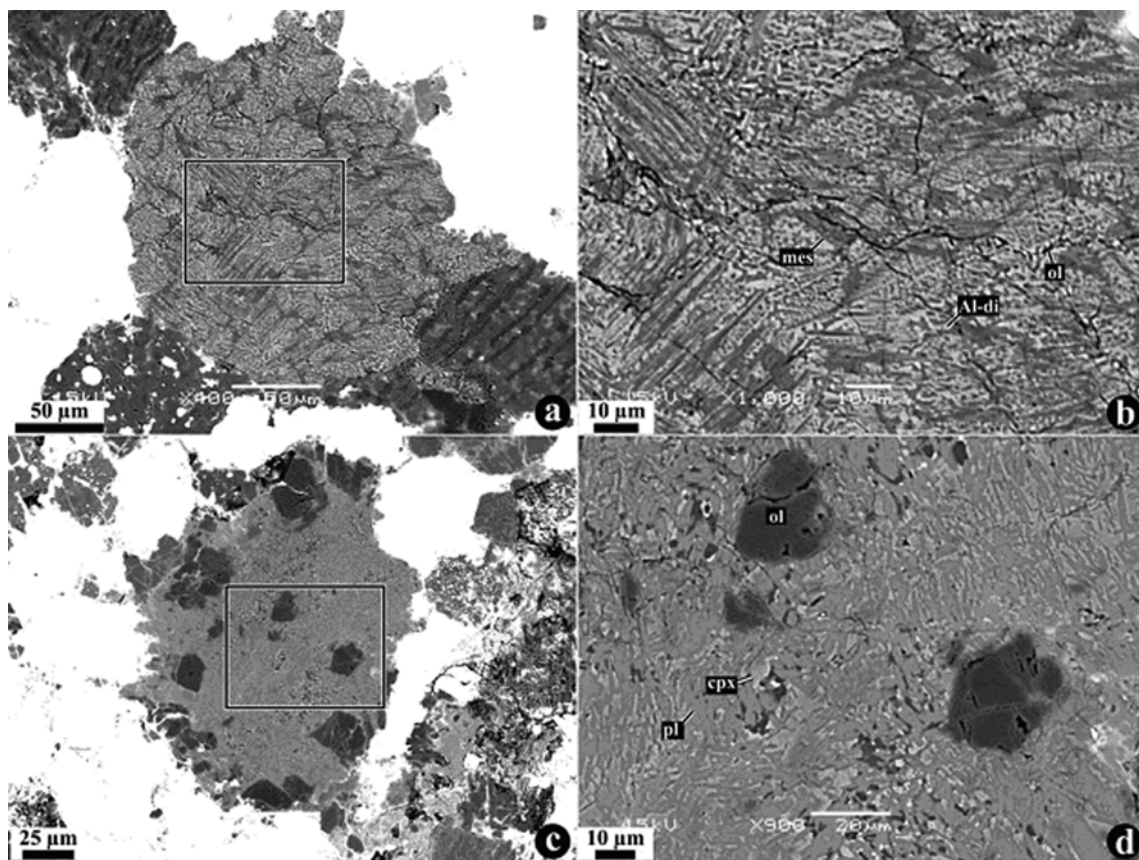


Fig. 10. BSE images of Al-rich chondrules from Isheyev. Regions outlined in (a) and (c) are shown in detail in (b) and (d), respectively. a, b) Al-diopside-rich chondrule. c, d) Plagioclase-rich chondrule. Al-di = Al-diopside; cpx = high-Ca pyroxene; mes = mesostasis; ol = olivine; pl = plagioclase.

of Pd are enriched by factor of  $\sim 7.8$ . The higher enrichments ( $13.7 \times$  CI and  $11.3 \times$  CI) have been reported for HaH 237 (Zipfel et al. 1998) and QUE 94411 (Weisberg et al. 2001). The volatile siderophile elements with condensation temperatures below Pd (e.g., Au, As, Cu) show volatility controlled depletions similar to those in QUE 94411, ALHA85085, Acfer 182, and NWA 470. Zn and Se contents are very depleted ( $0.24$  and  $0.15 \times$  CI, respectively).

#### Whole Rock Oxygen Isotopic Composition

The replicate analyses of two aliquots of homogenized material show good reproducibility, with  $\delta^{18}\text{O}$  values of  $4.2\text{\textperthousand}$  and  $4.3\text{\textperthousand}$  and  $\Delta^{17}\text{O}$  values of  $-1.0\text{\textperthousand}$  and  $-1.2\text{\textperthousand}$ ; the observed variations in  $\Delta^{17}\text{O}$  may indicate some isotopic heterogeneity within the samples. On a three-isotope oxygen diagram, the bulk compositions of two Isheyev samples analyzed plot close to the CR-mixing line, in the region of the CH and CB meteorites (Figs. 17a–b). The whole-rock oxygen isotopic compositions of the CH and CB meteorites clearly define two distinct groups, with the CB chondrites exhibiting a particularly narrow range in compositions with  $\Delta^{17}\text{O}$

around  $-2.3\text{\textperthousand}$  and  $\delta^{18}\text{O}$  restricted to a per mil or so either side of  $1.5\text{\textperthousand}$  (Weisberg et al. 1995; Clayton and Mayeda 1999; Grossman and Zipfel 2001; Russell et al. 2002). The CH chondrites display a wider range in  $\delta^{18}\text{O}$  values ( $-0.5\text{\textperthousand}$  to  $5.5\text{\textperthousand}$ ) with  $\Delta^{17}\text{O}$  values around  $-1.5\text{\textperthousand}$ . One CH chondrite, NWA 739, has a distinct  $\Delta^{17}\text{O}$  value of  $-0.5\text{\textperthousand}$ . The Isheyev samples are quite distinct from the CB chondrites, but do plot within the range of the CH chondrites, albeit towards rather extreme compositions for CHs. The only CH chondrites with  $\delta^{18}\text{O}$  values  $>3\text{\textperthousand}$  are the desert finds NWA 739 and Acfer 182. While the isotopic signature of these two meteorites may reflect isotopic heterogeneity in the CH parent body, the effect of terrestrial weathering in hot deserts cannot be excluded as this would have the effect of driving isotopic signatures to higher  $\delta^{18}\text{O}$  and  $\Delta^{17}\text{O}$ .

While the Isheyev oxygen isotopic composition is distinct from bulk O-isotopic compositions of CB chondrites, they do fall along a mixing line defined by samples of the shock-melted material from Bencubbin (Franchi et al. 1998). The  $^{16}\text{O}$ -depleted end-member of this mixing line is unknown—but clearly the possibility exists that there is some common relationship between this component, the metal-rich lithology silicates in Isheyev

Table 3. Representative chemical compositions of mineral phases from layered chondrules of Isheyev (in wt%).

Chondrule	C-29	C-29	C-40	C-40	C-42	C-42	C-43	C-43	C-43	C-11	C-11	C-14	C-14
Ol core	Phyrl rim	Opx core	Ol rim	Px core	Phyrl rim	Px core	Ol rim	Px core	Ol rim	Px core	Phyl rim	CC core	Ol rim
SiO <sub>2</sub>	40.1	38.4	55.3	34.0	55.00	34.3	55.2	34.0	29.4	58.1	33.4	50.5	31.7
TiO <sub>2</sub>	0.02	0.02	0.03	0.02	0.10	0.02	0.11	0.10	0.02	0.10	0.02	0.12	0.02
Al <sub>2</sub> O <sub>3</sub>	0.02	1.10	0.07	0.11	1.18	0.31	1.93	0.19	0.06	0.15	0.05	3.01	0.19
Cr <sub>2</sub> O <sub>3</sub>	0.69	0.51	0.74	0.03	0.82	0.20	0.68	0.26	0.01	0.58	0.10	0.71	0.14
FeO	12.9	34.0	15.6	48.4	1.19	43.0	9.34	51.5	59.2	4.94	47.0	13.5	54.4
MnO	2.12	0.58	0.14	0.46	0.19	0.16	0.11	0.35	0.59	0.05	0.12	0.20	0.84
MgO	44.5	9.70	29.2	17.5	40.46	7.26	30.8	14.5	9.51	36.8	5.22	29.7	11.9
CaO	0.15	1.45	0.10	0.16	1.05	0.90	1.41	0.37	0.47	0.16	1.28	2.45	0.63
Na <sub>2</sub> O	0.05	0.37	0.05	0.06	0.05	0.15	0.12	0.06	0.05	0.05	0.22	0.05	0.05
K <sub>2</sub> O	0.05	0.57	0.05	0.05	0.05	0.12	0.05	0.05	0.05	0.05	0.12	0.05	0.05
NiO	0.10	0.10	0.07	0.09	0.02	0.40	0.04	0.06	0.09	0.02	0.08	0.06	0.10
Total	100.8	86.9	101.3	100.9	100.1	86.8	99.8	101.4	99.4	100.9	87.7	100.3	100.1
Cations													
Si	1.00	1.97	1.00	1.88		1.94		1.01	0.95	1.97		1.83	0.98
Ti	0.00	0.00	0.00	0.00		0.00		0.00	0.00	0.00		0.00	0.00
Al	0.00	0.00	0.00	0.05		0.08		0.01	0.00	0.01		0.13	0.01
Cr	0.01	0.02	0.00	0.02		0.02		0.01	0.00	0.02		0.02	0.00
Fe	0.27	0.46	1.19	0.03		0.28		1.28	1.60	0.14		0.41	1.41
Mn	0.04	0.00	0.01	0.01		0.00		0.01	0.02	0.00		0.01	0.02
Mg	1.65	1.55	0.77	2.06		1.62		0.64	0.46	1.86		1.60	0.55
Ca	0.00	0.00	0.01	0.04		0.05		0.01	0.02	0.01		0.09	0.02
Na	0.00	0.00	0.00	0.00		0.01		0.00	0.00	0.00		0.00	0.00
K	0.00	0.00	0.00	0.00		0.00		0.00	0.00	0.00		0.00	0.00
Ni	0.00	0.00	0.00	0.00		0.00		0.00	0.00	0.00		0.00	0.00
Sum	2.99	4.02	3.00	4.09		4.01		2.98	3.05	4.02		4.10	3.01
Fs (mol%)													
Wo (mol%)	0.19	1.80		2.73				14.3		7.06		19.6	
En (mol%)	76.6	96.4		83.0						0.29		4.50	
Fa (mol%)	14.0	60.8								92.7		75.9	
													71.9

Abbreviations: Ol = olivine; Phyrl = phyllite; Opx = orthopyroxene; Phyl = phyllosilicate; CC = cryptocrystalline chondrule.

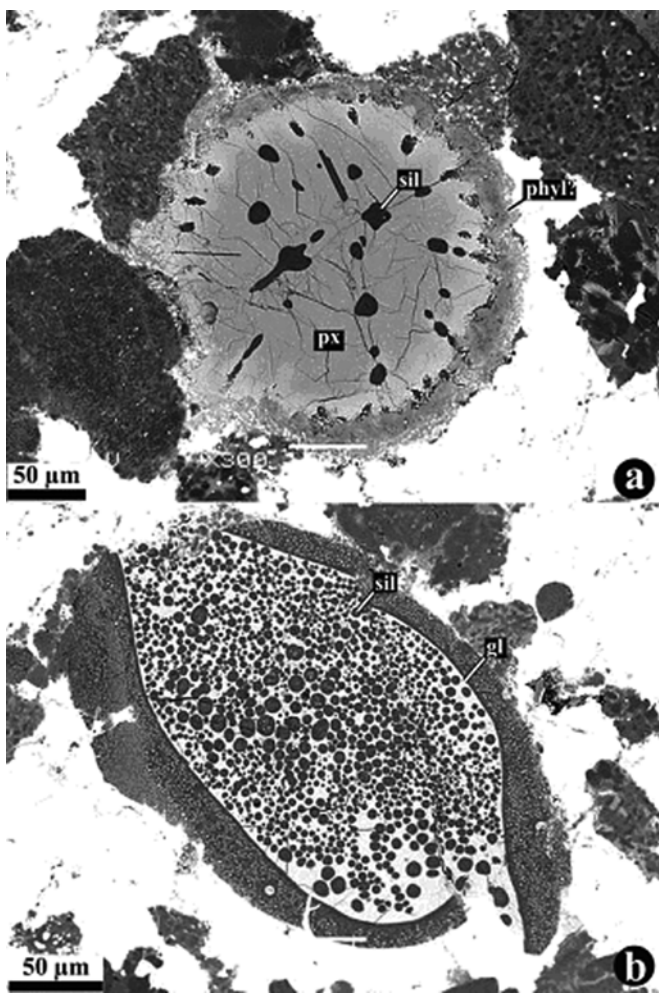


Fig. 11. BSE images of the silica-rich objects from Isheyev. a) Chondrule consists of silica (sil) and ferromagnesian pyroxene (px); it is surrounded by a very fine-grained material, possible hydrated alteration minerals (phyl). b) Ellipsoid object composed of numerous silica-rich spherules in ferromagnesian silicate glass (gl).

and possibly the hot desert CHs NWA 739 and/or Acfer 182.

#### Nitrogen and Carbon Isotopic Compositions

Nitrogen isotopic composition of the whole-rock sample of Isheyev (metal-rich lithology) is highly enriched in  $\delta^{15}\text{N}$ , reaching a peak  $\delta^{15}\text{N}$  value of 1523‰ around 1000 °C (Table 6; Fig. 18a). In terms of its overall nitrogen content, it contains 106 ppm nitrogen, with an average  $\delta^{15}\text{N}$  of 1122‰. This is the highest bulk  $\delta^{15}\text{N}$  value of any whole meteorite sample ever reported (Fig. 19 in Franchi et al. 1986; Grady and Pillinger 1990; Weisberg et al. 1995; Sugiura et al. 1999, 2000).

There is a bimodal release profile of  $\delta^{15}\text{N}$ , with the major peak coinciding with the peak in  $\delta^{15}\text{N}$  values. Below 600 °C there is a smaller release of nitrogen with lower enrichments in  $\delta^{15}\text{N}$ . The rising  $\delta^{15}\text{N}$  value across this release indicates

mixing of the high temperature isotopically heavy nitrogen with a second component of isotopically lighter nitrogen. The nature of this lighter component, with a  $\delta^{15}\text{N}$  value similar to terrestrial values is unknown—but may include a significant contribution from terrestrial contamination.

The release characteristics of the main component around 1000 °C is very similar to that observed in Bencubbin (e.g., Franchi et al. 1986), and is consistent with the nitrogen residing within Fe,Ni metal, or a more labile phase shielded by the Fe,Ni metal. Indeed, the magnetic fraction is very similar to the bulk sample in terms of both nitrogen release pattern and isotope profile (Fig. 18b), and contains a similar concentration of nitrogen (113 ppm) with a comparable  $\delta^{15}\text{N}$  value (1056‰). The non-magnetic fraction, largely free of Fe,Ni metal, contains more nitrogen (189 ppm) than the whole-rock or magnetic fraction. However, almost all of this nitrogen is liberated at low temperatures (<600 °C) and is associated with a broad carbon peak, and has a much lower bulk  $\delta^{15}\text{N}$  value (214‰, Fig. 18c). This component is clearly associated with the silicate portion, possibly the hydrated lithic fragments, although this would suggest that they are particularly carbon rich, as the non-magnetic fraction contains 1.1 wt% C. The same component is apparent, at reduced levels, in the whole-rock and magnetic fraction.

In all the fractions analyzed, the heavy nitrogen is decoupled from the carbon release (Figs. 18d–f; Table 6). The vast bulk of the carbon found in Isheyev is released at low temperatures. The initial steps in all three samples have  $\delta^{13}\text{C}$  values starting around -25‰, indicative of terrestrial contamination, but at 500 °C the  $\delta^{13}\text{C}$  values are around 0‰, much more typical of indigenous carbon. There is insufficient temperature step resolution to determine if any of the carbon is directly related to N release at low temperatures. However, the C/N ratio ~65 is intermediate between typical carbonaceous chondrite macromolecule and terrestrial contamination, suggesting that both are contributing to the large release. At high temperatures there is no evidence for a significant carbon release associated with the large release of isotopically heavy nitrogen, although the carbon isotope signature does peak around 1000 °C in the whole-rock and magnetic fractions with  $\delta^{13}\text{C} \sim 7\text{‰}$  (Figs. 18d and e).

#### $^{40}\text{Ar}$ - $^{39}\text{Ar}$ Dating

The  $^{40}\text{Ar}$ - $^{39}\text{Ar}$  age spectrum of Isheyev is shown in Fig. 20. Similar to most other primitive, chondrites, there is no simple plateau-shaped age spectrum, but a rather complicated irregular spectrum, with very high apparent ages in initial temperature extractions—partly exceeding the age of the solar system—and decreasing ages at high temperature extractions. This feature is an artifact related to the primitive fine-grained mineral assemblage, particular of the potassium-bearing phases, which are about micrometer-sized phyllosilicates. Fine-grained potassium carrier phases facilitate disturbances by both

secondary  $^{40}\text{Ar}$  loss due to later reheating processes and also  $^{39}\text{Ar}$  redistribution by recoil, due to the ( $n, p$ ) reaction converting  $^{39}\text{K}$  to  $^{39}\text{Ar}$  during neutron irradiation. This reaction typically causes a  $^{39}\text{Ar}$  deficit in potassium-phase grain boundaries, from which it is efficiently lost into neighboring potassium-poor minerals such as pyroxene and olivine. These minerals release  $^{39}\text{Ar}$  at high temperatures only, causing unrealistically low apparent ages. On the other hand, the  $^{39}\text{Ar}$  deficit in potassium-phase grain boundaries causes unrealistically high apparent ages at low extraction temperatures. This leads to age spectra with high apparent ages in the first extractions, followed by decreasing apparent ages in the high temperature extractions. A prominent example of this type is the Tieschitz (H3.4) age spectrum measured by Turner et al. (1978). The total K-Ar age of the Isheyev sample is ~4.3 Ga, i.e., close to the to the age of the solar system.

Furthermore, we observe a significant trapped argon component (with  $^{36}\text{Ar}/^{38}\text{Ar} = 5.35$ , deconvolved from cosmogenic argon with  $^{36}\text{Ar}/^{38}\text{Ar} = 0.65$ ) in each temperature extraction. An isochron plot constructed with trapped  $^{36}\text{Ar}$  is shown in Fig. 21. In the first two low-temperature extractions, this trapped argon could be of terrestrial atmospheric origin (pointing to an y-axis intercept with  $^{40}\text{Ar}/^{36}\text{Ar} = 295.5$ ) possibly residing in alteration products. At high extraction temperatures, still significant amounts of trapped argon are released, but of extraterrestrial origin, with  $^{40}\text{Ar}/^{36}\text{Ar}$  ratios  $<3.4$ . Two distinct trapped components of terrestrial and non-terrestrial origin is also found in other chondrites (Korochantseva et al. 2007).

Besides trapped argon, there is a cosmogenic argon component (with  $^{36}\text{Ar}/^{38}\text{Ar} = 0.65$ ) produced during recent exposure to galactic cosmic rays, before the meteorite reached the Earth as meter-sized body. Based on concentration of cosmogenic  $^{38}\text{Ar}$  which is ~38% of total  $^{38}\text{Ar}$  and using a production rate of  $6.75 \times 10^{-10} \text{ }^{38}\text{Ar}$  (cm $^3$  STP/g per Ma), we calculate a cosmic-ray exposure age of 34 Ma (Table 7).

## DISCUSSION

### Metal-Poor and Metal-Rich Lithologies: Connection to the CH and CB<sub>b</sub> Chondrites?

Isheyev is a unique metal-rich carbonaceous chondrite containing several lithologies: metal-poor (#1 and #2), and metal-rich (#3 and #4). Similarly to CH and CB<sub>b</sub> chondrites, Isheyev lacks interchondrule fine-grained matrix material and contains abundant metal-free, magnesian, skeletal, and cryptocrystalline chondrules, irregularly shaped Fe,Ni-metal grains, very refractory inclusions and heavily hydrated lithic clasts. There are significant variations in chemical compositions between individual metal grains; Co/Ni ratio is nearly solar. About 20–30% of metal grains are chemically

zoned with Ni and Co decreasing and Cr increasing from core to rim of the grains. This zoning is consistent with a gas-solid condensation origin (e.g., Meibom et al. 1999; Campbell et al. 2001; Petaev et al. 2001). Some of the compositionally uniform metal grains contain rounded inclusions of Cr-bearing sulfides. Similar to QUE 94411 and HaH 237, Isheyev contains thin films of impact melts separating coarse silicate and metal components (Meibom et al. 2005).

The Isheyev refractory inclusions are texturally, mineralogically, and chemically similar to those in CH chondrites and to a lesser degree to those in the CB<sub>b</sub> chondrites (Krot et al. 2006b, 2007b, 2007c); AOAs are very rare. CAIs are dominated by hibonite, grossite, perovskite, and gehlenitic melilite, and show little evidence for replacement by low-temperature minerals, such as Al-diopside and anorthite, possibly indicating a short residence time of the CAIs in the low-temperature condensation region. Most CAIs appear to have been melted. In contrast to the Isheyev CAIs, those in CB<sub>b</sub> chondrites are dominated by the igneous, spinel-pyroxene-melilite CAIs, which are typically surrounded by a monomineralic layer of forsterite (Krot et al. 2001b). We note that some CAIs in Isheyev are similar to those found in CB<sub>b</sub> chondrites, but such CAIs are not dominant (Krot et al. 2006c).

Based on these observations, as well as bulk chemical, oxygen, and nitrogen isotopic similarities to the CH and CB<sub>b</sub> chondrites, we infer that Isheyev is a CH/CB<sub>b</sub>-like meteorite. Currently, it is the only metal-rich carbonaceous chondrite containing different lithologies. We note, however, that CBa and CB<sub>b</sub> subgroups may also represent different lithologies of the same parent asteroid (Krot et al. 2005).

There are petrographic and mineralogical similarities between the metal-poor and metal-rich lithologies of Isheyev and CH and CB<sub>b</sub> chondrites, respectively; although, there are some significant differences as well. Contrary to CH chondrites, the average chondrule sizes of which 0.02–0.09 mm (Weisberg et al. 1995), the metal-poor lithology is coarser grained, with the average size of chondrules 0.40 mm. This lithology also contains more abundant zoned Fe,Ni-metal grains than CH chondrites. Silica-rich spherules, and ferrous cryptocrystalline spherules with euhedral metal grains commonly observed in CH chondrites (Krot et al. 2000; Hezel et al. 2003), are very rare in Isheyev.

In contrast to CB<sub>b</sub> chondrites (with chondrule sizes from 0.30 to 1 cm [Zipfel et al. 1998; Weisberg et al. 2001]), the metal-rich lithology of Isheyev is finer grained, with the average size of chondrules 0.10 mm, and contains abundant porphyritic chondrules, as well as ferrous chondrules and chondrules rich in Fe,Ni metal and silica. In addition, Ni-rich metal grains commonly observed in Isheyev are not found in CB<sub>b</sub> chondrites (Campbell et al. 2001; Meibom et al. 2001; Petaev et al. 2001).

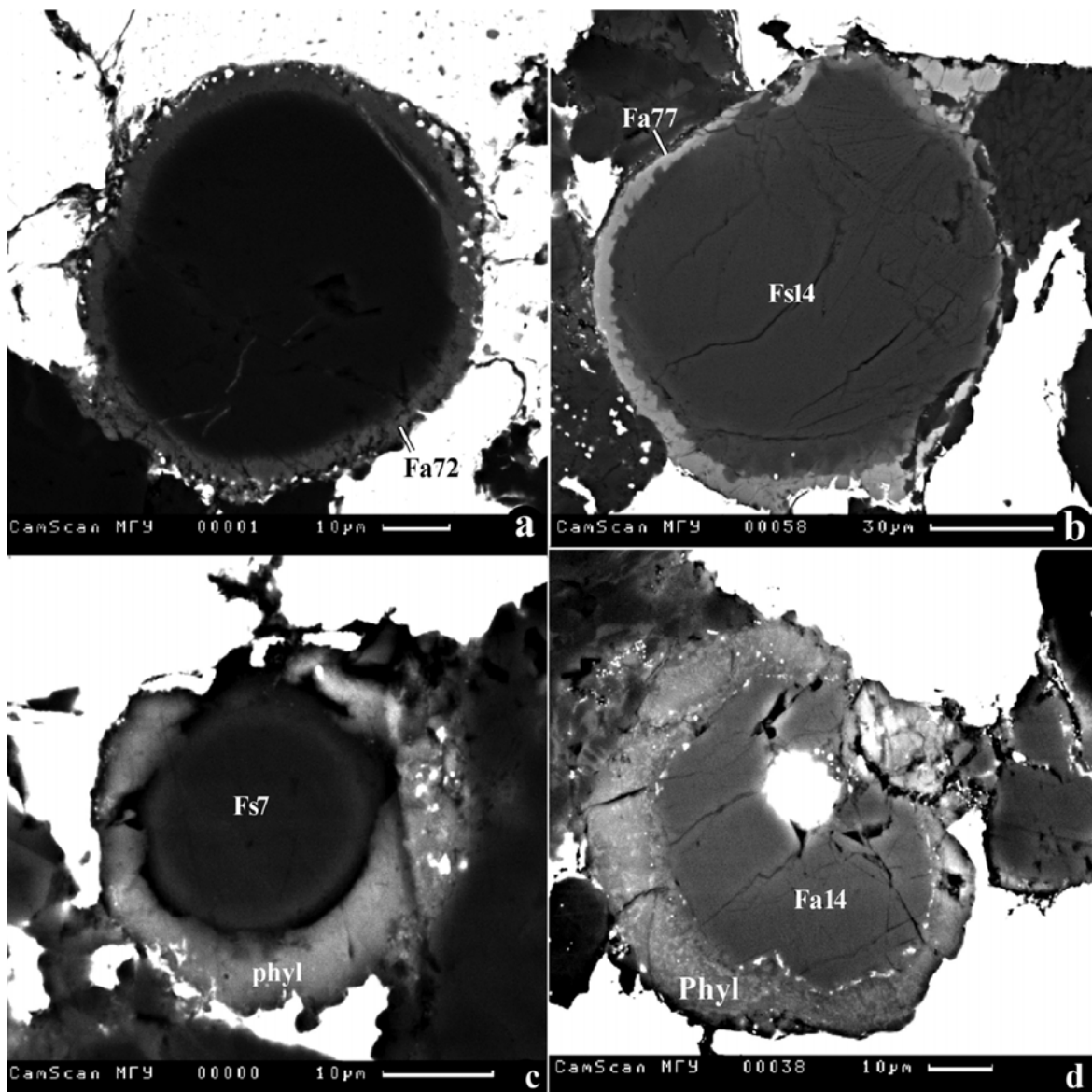


Fig. 12. BSE images of the layered chondrules from Isheyev: C-14 (a), C-43 (b), C-11 (c), C-29 (d). The chondrules consist of ferromagnesian pyroxene (b, c) or olivine (d); they are rimmed either by fayalitic olivine ( $\text{Fa}_{60-72}$ ) (a, b) or phyllosilicates (phyl) (c, d).

Bulk lithophile and siderophile element abundances of Isheyev have similar volatility-controlled patterns to those of the CH and CB chondrites, suggesting common formation mechanism, possibly by fractional condensation. The observed similarities in bulk oxygen and nitrogen isotopic compositions of Isheyev, CH, and CB chondrites are consistent with their derivation from a common reservoir. However, there are small but consistent differences in the whole-rock oxygen isotopic composition of the CH and CB chondrites, and Isheyev is distinct from the CB chondrites. Whether Isheyev falls within the field of the CH chondrites may be somewhat complicated by the unquantified effects of terrestrial weathering in some meteorites. However, the differences between all these metal-rich meteorites are small

and most likely point to local variations acting on a common reservoir rather than different sources.

Isheyev appears to contain a very similar or possibly the same carrier of the heavy nitrogen as found in Bencubbin (Franchi et al. 1986). The nature of the heavy nitrogen carrier in Isheyev has not been established, although it has been argued that in Bencubbin the main nitrogen component resides in carbides or taenite associated with Cr-rich sulfides (Sugiura et al. 2000) as identified by secondary ionization mass-spectrometry (SIMS). However, the stepped combustion data argue against such phases being the major hosts. The very low C/N ratio observed in acid residues strongly argues against carbide being the host phase while the fact that essentially all the nitrogen is retained in a 6M HCl residue (Franchi et al.

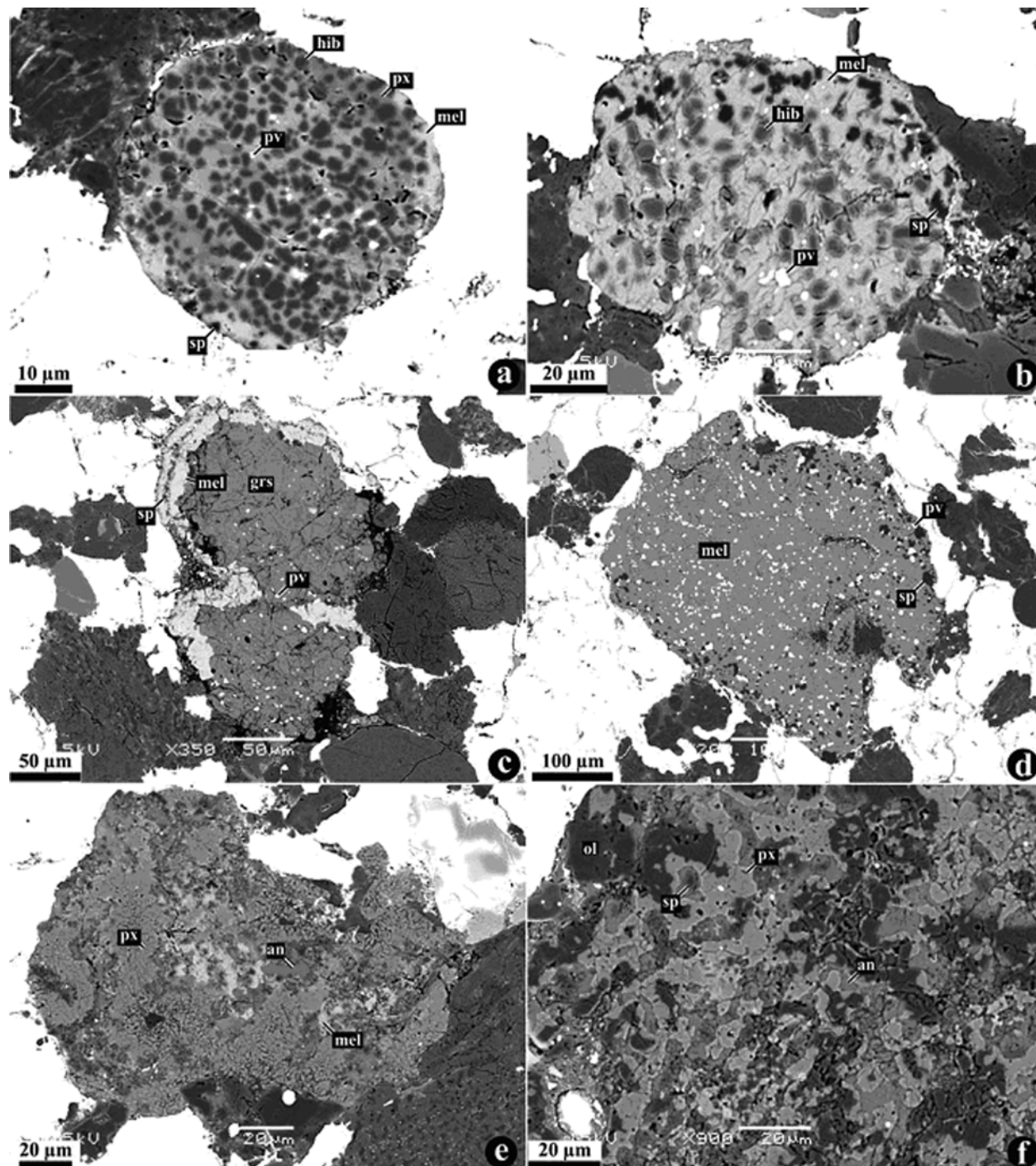


Fig. 13. BSE images of two populations of refractory inclusions from Isheyev. a–c) Very refractory, compact CAIs composed of hibonite, grossite, Al-rich pyroxene, gehlenitic melilite, perovskite, and minor spinel. Secondary anorthite and Al-diopside are absent. d–f) Less refractory inclusions composed of melilite, spinel, Al-diopside, forsterite, and anorthite. an = anorthite; ol = olivine; sp = spinel; grs = grossite; hib = hibonite; mel = melilite; pv = perovskite; px = Al-pyroxene.

1986) argues against taenite as a possible host. Sugiura et al. (2000) argued that nitrogen in Bencubbin had been remobilized during the shock melting event, which may also account for the lack of any associated primordial gases in the acid residues (Rooke et al. 1998). Given the levels of high level of shock metamorphism experienced by Isheyev, this

explanation is most likely, given the strong similarity in nitrogen isotopic systematics and release profile. We mentioned that the nature of the lighter component of N, with a  $\delta^{15}\text{N}$  value similar to terrestrial values is unknown, but may include a significant contribution from terrestrial contamination. Other possible sources of light nitrogen may include the hydrated

Table 4. Chemical compositions of CAIs and Al-rich chondrules from Isheyev (in wt%).

N	Type	SiO <sub>2</sub>	TiO <sub>2</sub>	Al <sub>2</sub> O <sub>3</sub>	Cr <sub>2</sub> O <sub>3</sub>	FeO	MnO	MgO	CaO	Total
CAI1b	Sp-Mel-Di-Pv	7.71	3.90	56.4	0.05	0.84	0.02	20.0	10.0	98.92
CAI2b	Grs-Di-An-Pv	19.2	2.38	51.0	0.09	2.04	<0.02	1.08	23.3	99.09
CAI16-2b	Grs-Mel-Di-Pv	5.96	5.67	62.1	0.02	0.44	<0.02	0.60	24.4	98.59
CAI16-1b	Grs-Mel-Pv	18.9	1.03	42.4	0.04	1.30	0.02	1.96	33.2	98.85
CAI24b	Grs-Mel-Pv	13.0	1.91	49.6	0.05	2.80	<0.02	1.08	29.7	98.14
CAI25b	Sp-Mel-Di	17.0	0.18	46.4	0.12	2.03	<0.02	19.6	15.3	100.6
CAI22b	Grs-Mel-Pv	12.8	2.45	49.9	<0.02	0.99	0.02	0.10	32.8	98.96
CAI11b	Mel-Sp	20.9	0.85	34.9	<0.02	5.29	0.03	2.01	34.9	98.88
CAI10s	Grs-Mel-Pv	1.30	2.22	71.1	0.04	0.31	<0.02	1.98	21.7	98.65
CAI12s	Grs-Mel-Pv	0.05	5.30	66.9	<0.02	2.98	0.02	0.89	23.0	99.94
CAI14s	Mel-Sp	18.1	0.65	41.5	0.04	2.54	0.02	9.26	27.8	99.91
CAI15s	Grs-Pv-Mel	0.07	4.95	71.5	<0.02	0.46	<0.02	0.43	23.0	100.4
CAI1s	Mel-Sp-Pv-Di	19.8	4.95	31.2	<0.02	0.54	<0.02	1.27	40.4	98.16
CAI9s	Sp-Di	17.4	3.31	57.3	0.07	0.60	0.02	4.02	18.7	101.5
CAI7s	Grs-Mel-Pv	14.7	3.42	45.0	<0.02	0.63	<0.02	1.62	34.3	99.67
CAI6s	Mel-Grs-Pv	15.1	1.42	48.4	0.06	2.08	0.03	2.15	30.1	99.34
CAI4s	Hib-Grs-Pv-Sp-Di	7.56	2.86	59.6	0.03	2.25	0.02	4.74	21.8	98.86
45	Al-rich chondrule	44.6	0.91	18.0	0.13	1.69	0.06	17.3	15.4	98.09
44	Al-rich chondrule	42.4	0.58	15.9	0.24	2.05	<0.02	25.9	12.7	99.77

Abbreviations: Sp = spinel; Mel = melilite; Di = diopside; Pv = perovskite; Grs = grossite; Hib = hibonite.

Table 5. Bulk chemical compositions of Isheyev and NWA 470.

Element	Isheyev	NWA 470
Hf, ppm	0.058 ± 0.01	0.39
Al, wt%	0.51 ± 0.002	0.95
Sc, ppm	4.20 ± 0.4	5.69
Lu, ppm	0.018 ± 0.003	0.037
Tb, ppm	0.020 ± 0.004	0.10
Ti, ppm	264 ± 2	0.05
La, ppm	0.25 ± 0.01	0.37
Ca, wt%	0.600 ± 0.002	1.33
V, ppm	52.1 ± 0.5	
Sm, ppm	0.11 ± 0.03	0.37
Nd, ppm	0.36 ± 0.02	1.18
Ce, ppm	0.460 ± 0.001	0.84
Yb, ppm	0.12 ± 0.02	0.202
Eu, ppm	0.043 ± 0.01	0.037
Mg, wt%	5.830 ± 0.002	10.34
Si, wt%	6.140	11.19
Cr, wt%	0.25 ± 0.0003	0.41
Mn, ppm	520 ± 0.1	0.08
K, ppm	45 ± 14	0.04
Na, ppm	263 ± 11	0.18
Zn, ppm	45 ± 0.07	
Se, ppm	1.63 ± 0.4	2.23
Ir, ppm	2.6 ± 0.17	
Ni, wt%	5.10 ± 0.0001	3.26
Co, ppm	2100 ± 0.02	0.15
Fe, wt%	87.02 ± 0.0004	44.38
Pd, ppm	2.32 ± 0.05	
Au, ppm	0.23 ± 0.01	0.14
As, ppm	1.21 ± 0.4	3.15
Cu, ppm	78.0 ± 0.2	90.0
S, wt%	0.52	0.64
H <sub>2</sub> O, wt%	0.49	3.00

lithic clasts, analogous to the hydrated areas in Pecora Escarpment (PCA) 91467 containing similar enrichments of <sup>15</sup>N as measured by SIMS.

### Origin of Chondritic Components of Isheyev

#### Chondrules and CAIs

It appears that there are probably at least two populations of chondrules in Isheyev: 1) non-porphyritic magnesian and 2) porphyritic ferromagnesian, Al-rich and silica-rich. The magnesian non-porphyritic chondrules are texturally and mineralogically similar to those in CB and CH chondrites. Chondrules of similar textures and compositions are sometimes found inside Fe,Ni-metal condensates and have rather unique textures and mineralogies not observed in other chondrite groups (Krot et al. 2005, 2006b). They show no evidence for remelting, i.e., contain no relict grains, do not form independent compound chondrules, and are not surrounded by coarse-grained igneous rims. It has been previously concluded that such chondrules in CB chondrites formed from a gas-melt plume generated during a single-stage process, possibly during a large-scale collision between planetary embryos (Krot et al. 2005). However the chondrules could have formed in the solar accretion disk, and the absence of recycling among CB<sub>b</sub> chondrules might be an evidence for the exhaustion of the energy source for making chondrules (Gounelle et al. 2007). Without knowledge of the absolute ages of the Isheyev non-porphyritic magnesian chondrules and their oxygen isotopic compositions, it is difficult to infer their genetic relationship to CB chondrules, although based on their unique mineralogical and petrographic characteristics, we suggest that these chondrules may have formed by a similar process, possibly even during, the same event.

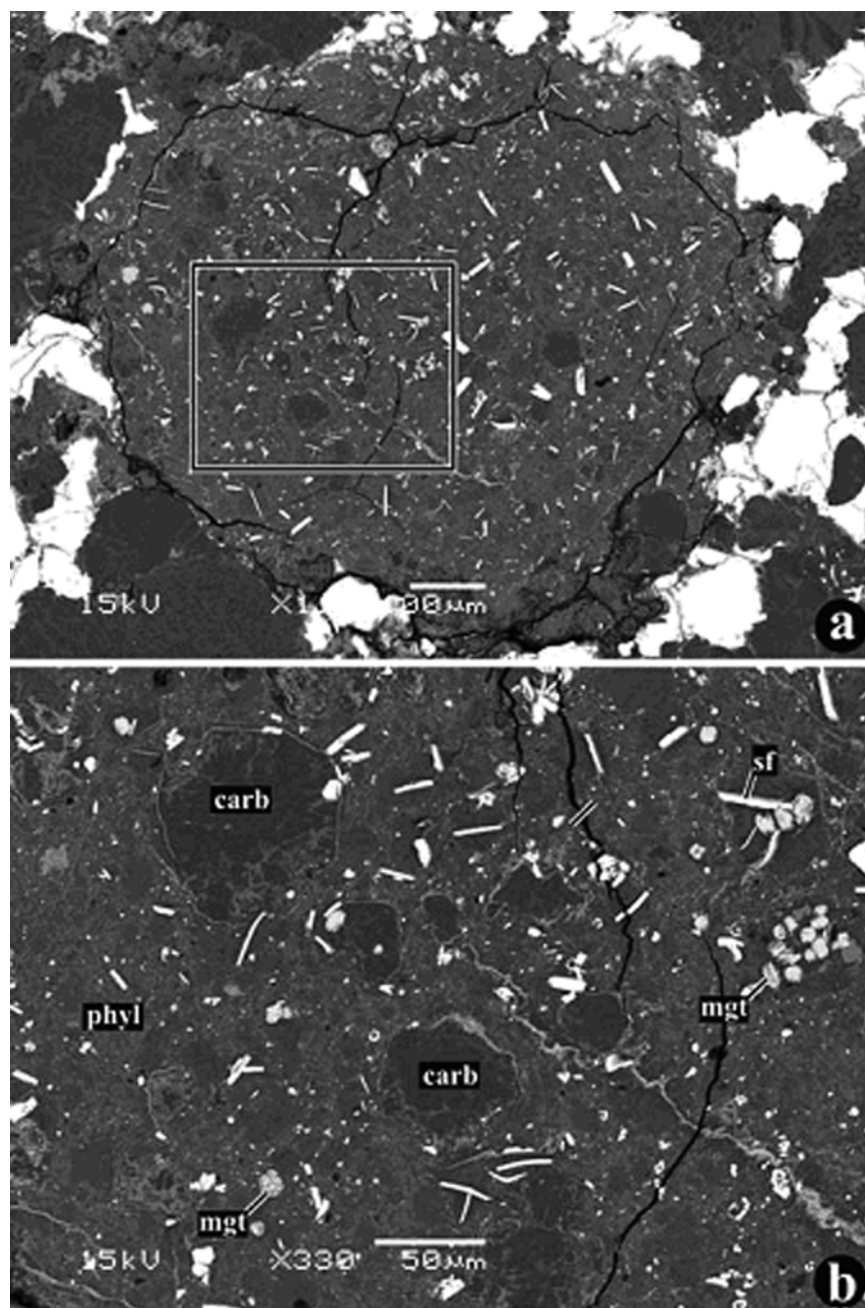


Fig. 14. BSE images of a heavily hydrated lithic clast from Isheyev. Region outlined in (a) is shown in detail in (b). The clast is composed of coarse-grained Ca-carbonate (carb), lath-shaped sulfides (sf), frambooidal and platy magnetite (mgt), and phyllosilicate (phyl) groundmass.

The Isheyev porphyritic chondrules are petrographically and mineralogically similar to those from other ordinary and carbonaceous chondrites, which are commonly believed to have formed from incomplete melting of solid precursors (e.g., Jones et al. 2005 and references therein). The rare occurrences of porphyritic chondrules with relict CAIs and relict ferromagnesian silicates, possibly representing fragments of earlier generations of chondrules, support this conclusion (Krot et al. 2006b,c 2007a). Based on the sizes of porphyritic chondrules, the rare occurrences of

type II chondrules, the lack of coarse-grained igneous rims, and the presence of very metal-rich type I chondrules, a relationship to chondrules in CV, CK, CR, CM, and CO chondrites can be probably eliminated, suggesting that these chondrules form their own population, i.e., they originated in their own chondrule-forming region. Although it seems unlikely that these chondrules formed during the same event that produced magnesian non-porphyritic chondrules and isolated Fe,Ni-metal grains, they might represent the precursor material for the former. Oxygen and magnesium

Table 6. Carbon and nitrogen isotopic compositions in the whole rock, magnetic, and non-magnetic fractions of Isheyev.

Temperature (°C)	Whole rock				Magnetic fraction				Non-magnetic fraction			
	C ppm	$\delta^{13}\text{C}$ ‰	N ppm	$\delta^{15}\text{N}$ ‰	C ppm	$\delta^{13}\text{C}$ ‰	N ppm	$\delta^{15}\text{N}$ ‰	C ppm	$\delta^{13}\text{C}$ ‰	N ppm	$\delta^{15}\text{N}$ ‰
200	112	-27.8	1.8	124	163	-23	0.68	46	628	-26	4.6	26
300	535	-16.1	2.4	198	518	-16	5.5	156	2404	-22	32	37
400	794	-3.6	5.4	514	628	-3.5	7.9	472	3310	-14	53	131
500	822	0.1	13	654	432	0.84	14	601	2934	-4.3	57	263
600	613	3.3	11	753	366	2.5	9.6	713	1754	1.1	29	362
700	301	3.7	5.3	866	249	4.3	7	820	402	0.75	6.1	494
800	231	5.1	5.8	907	250	6	6.7	975	108	-3.4	3.2	516
900	159	6.1	6.8	1100	194	7.8	19	1373	47	-2.9	2.1	626
1000	82	6.9	33	1516	123	8.1	19	1427	36	-9.1	0.78	527
1100	18	5.6	20	1510	56	4	20	1479	11	-7.1	0.64	206
1200	3	2.8	1.5	1004	6	-0.75	3	1554	9	-2.9	0.49	205
1300	5	3	0.63	523	14	-19	1	216	11	-6.5	0.68	176
1400	2	-17.9	0.32	183	3	-22	0.22	102	7	-20	0.29	78
Total	3680	-2.3	106	1124	3010	-2.8	113	1056	11670	-11	189	213

Table 7. Concentrations of trapped argon ( $^{36}\text{Ar}_t$ ), cosmic ray exposure ages (CRE ages) and  $^{40}\text{Ar}$ - $^{39}\text{Ar}$  ages of Isheyev, Bencubbin and CH chondrites.

	Isheyev	HaH 237	PAT 91546	PCA 91468	RKP 92435	Bencubbin
$^{36}\text{Ar}_t$	19.6	55.3	49.0	53.0	50.4	
CRE ages (Ma)	34	>3	>8	4.3	1.5	$39 \pm 3$
$^{40}\text{Ar}$ - $^{39}\text{Ar}$ ages (Ga)	<3.5	-	-	-	-	3.7-4.0

Concentrations of trapped argon are in  $10^{-8}\text{cm}^3\text{STP/g}$ . Data for Bencubbin from Kelly and Turner (1987), for HaH 237, PAT 91546, PCA 91468, RKP 92435 from Weber et al. (2001).

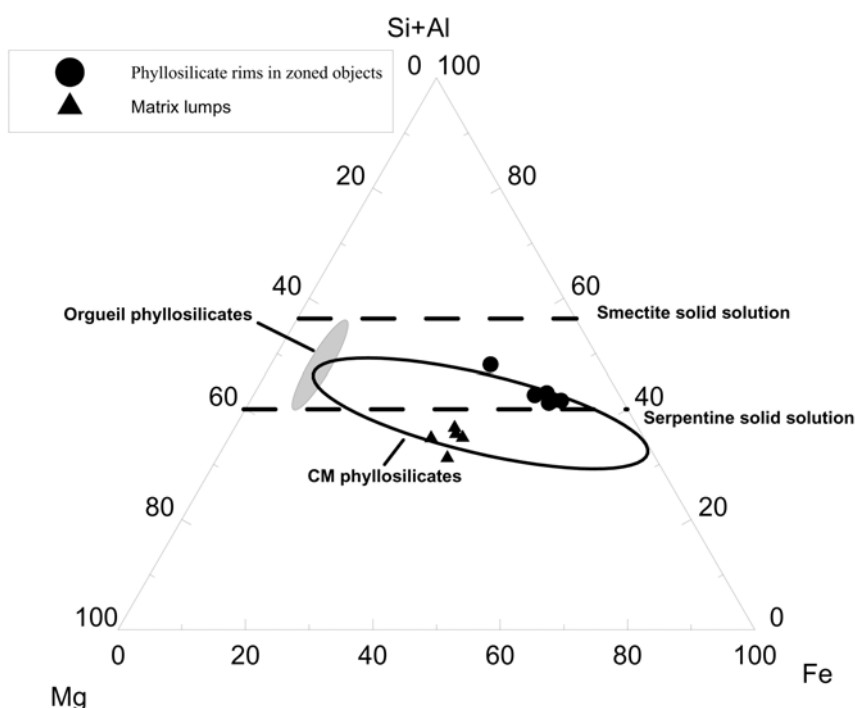


Fig. 15. Fe-(Si + Al)-Mg diagram of chemical compositions of phyllosilicates in layered chondrules and heavily hydrated lithic clasts from Isheyev. Compositional fields of phyllosilicates from CM chondrites and CI chondrite Orgueil (McSween and Richardson [1977]) are shown for comparison.

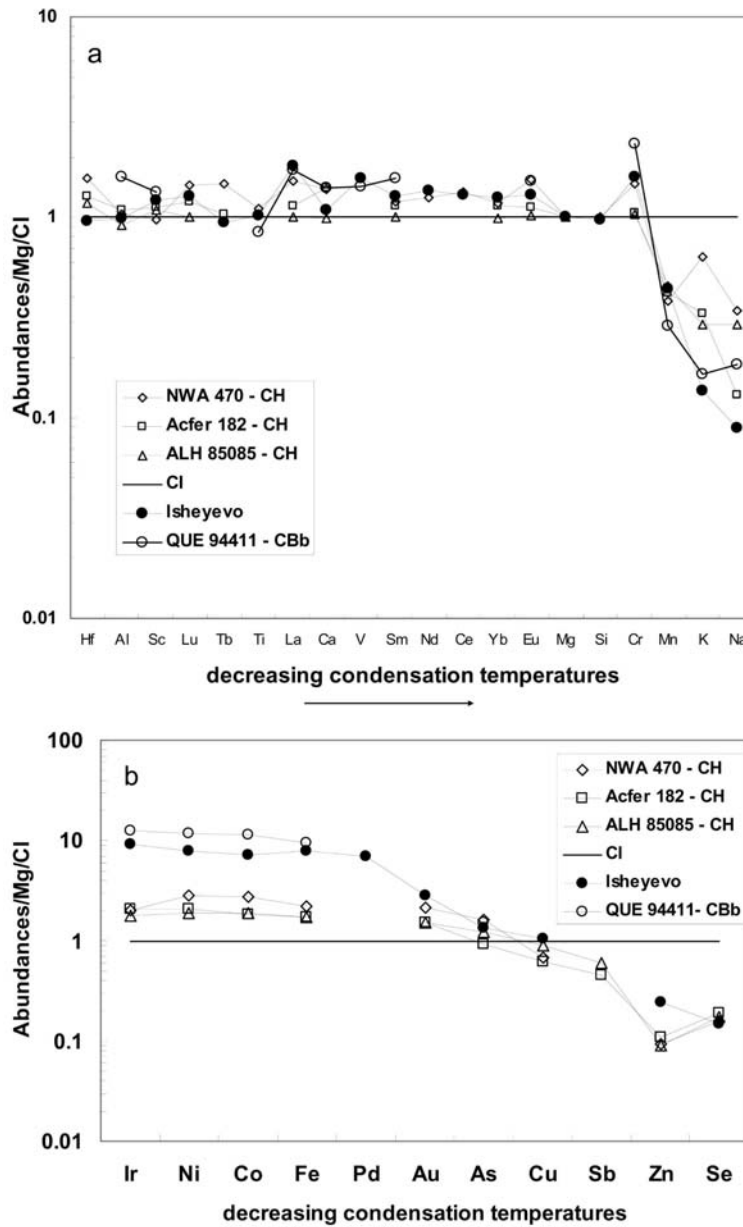


Fig. 16. CI and Mg normalized lithophile (a) and siderophile (b) element abundance patterns of Isheyev, CH chondrites NWA 470 (Table 4), Acfer 182, and ALH 85085, and CB<sub>b</sub> chondrite QUE 94411. Data from Wasson and Kallemeyn (1990), Bischoff et al. (1993a), Weisberg et al. (2001). Elemental abundances for CI chondrites are from Anders and Grevese (1989).

isotopic compositions of the Isheyev chondrules may be able to provide tests of these hypotheses.

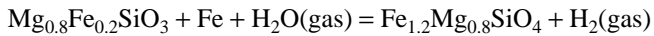
Our mineralogical observations may indicate that there are two populations of CAIs in Isheyev. One of them is a population of very refractory inclusions (grossite- and hibonite-rich) that appear to have crystallized from rapidly cooling melt. The general lack of secondary anorthite replacing melilite in these inclusions may indicate that they experienced only limited degree of interaction with cooling nebular gas at temperatures of anorthite condensation, possibly as a result fast removal from the high-temperature

nebular region. These inclusions are distinct from CAIs in other carbonaceous chondrite groups.

Another population of CAIs is less refractory inclusions commonly showing evidence for gas-solid interaction: e.g., replacement of melilite and spinel by secondary anorthite and Al-diopside, and formation of Wark-Lowering rims. These CAIs are texturally and mineralogically similar to those in other chondrite groups. Based on the different inferred initial  $^{26}\text{Al}/^{27}\text{Al}$  ratios ( $\sim 5 \times 10^{-5}$  and  $\sim 5 \times 10^{-7}$ ) in these populations of CAIs, Krot et al. (2007a, 2007b, 2007c) concluded that they represent two generations of refractory inclusions.

### Layered Chondrules and Lithic Clasts

Similar to CH chondrites, Isheyev contains mineralogically zoned (layered) chondrules and heavily hydrated lithic clasts. The layered chondrules are found only in the metal-rich lithologies (Fig. 12). They have magnesium-rich, pyroxene-normative cores surrounded by ferrous olivine rims suggesting formation under variable redox conditions, with extremely oxidizing conditions established at the end of their formation (Ivanova et al. 2001). Such conditions could have been generated by evaporation of dust-enriched regions or regions with high abundance of water ice particles (Ebel and Grossman 2000):



The presence of water ice might be consistent with the presence of ferrous phyllosilicate rims around some of the magnesian, cryptocrystalline spherules. It is unclear whether such chondrules formed during multistage processing of dust or whether they were produced during a single event in a region with variable redox conditions (Ivanova et al. 2001). Phyllosilicate rims may have formed by replacement of fayalitic olivine rims in an icy region of the nebula by their reaction with impact-generated water vapor as proposed by Ciesla et al. (2003). Alternatively, these chondrules originated on an asteroidal body that experienced incipient aqueous alteration and subsequently accreted together with other Isheyev components. However, the absence of chondrules in heavily hydrated lithic clasts probably excludes hydration of layered chondrules on the same parent body. Chemical compositions of the phyllosilicate rims and phyllosilicates from the hydrated lithic clasts are different: the former are more FeO-rich (Fig. 15), which could support formation of phyllosilicate rims from fayalitic olivine rims.

Heavily hydrated lithic clasts most likely experienced aqueous alteration in an asteroidal setting and later accreted together with other chondritic components into the Isheyev parent body. There is no evidence that these clasts could have originated in an impact plume inferred by Krot et al. (2005).

### $^{40}\text{Ar}$ - $^{39}\text{Ar}$ Age, Shock Metamorphism and Cosmic Ray Exposure Age

One of the major problems with the type of age spectra displayed by Isheyev (Fig. 20) or other fine-grained chondritic meteorites (Turner et al. 1978) is that recognition of secondary  $^{40}\text{Ar}$  loss by reheating processes is quite difficult. A possible  $^{40}\text{Ar}$  loss from potassium-bearing phase grain boundaries would be recognizable by low apparent ages at low extraction temperatures; however, this effect could be overruled by  $^{39}\text{Ar}$  recoil loss (causing the opposite effect). Therefore we need informations in addition to the mere shape of the age spectrum. Considering that the total K-Ar age of 4.3 Ga is close to the age of the solar system—Nakashima et al. (2006) obtained a very similar value of 4.4 Ga—the shape

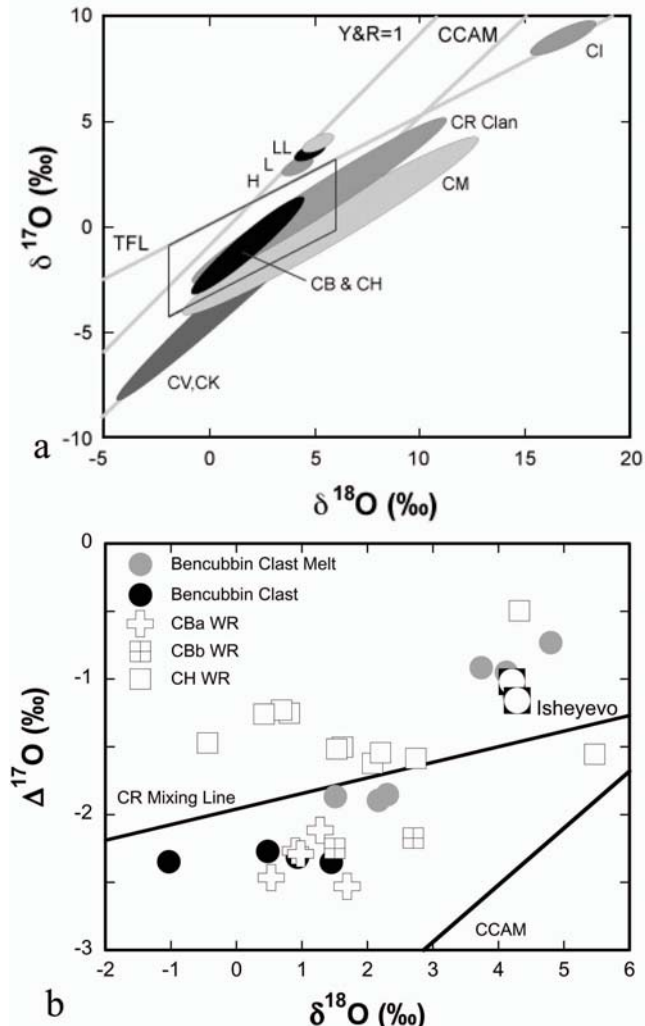


Fig. 17. a) Bulk oxygen isotopic compositions of CR, CH, and CB chondrites. b) Data from Clayton and Mayeda 1999; Weisberg et al. 2001; Franchi et al. 1998, and Isheyev (this study).

of the Ar-Ar age spectrum could be solely ascribed to the  $^{39}\text{Ar}$  recoil artifact. In this case there would be no major reheating effects causing secondary  $^{40}\text{Ar}$  loss after  $4.3 \pm 0.1$  Ga ago. The Ar-Ar age would reflect the last major event possibly being a large giant impact soon (about a few Ma) after or in the course of the formation of the Isheyev parent body (Krot et al. 2005).

On the other hand, the K-Ar age could be younger, as we possibly have some trapped terrestrial argon in the low temperature extractions (Fig. 21). If this is indeed the case, then terrestrial argon has to be subtracted when calculating the K-Ar age, and the latter would be lowered. This could imply secondary  $^{40}\text{Ar}$  loss, possible as late as  $<3.5$  Ga ago, as judged from the maximum age of the medium temperature extractions, that are presumably unaffected by trapped terrestrial argon.

Secondary events such as impact metamorphism have

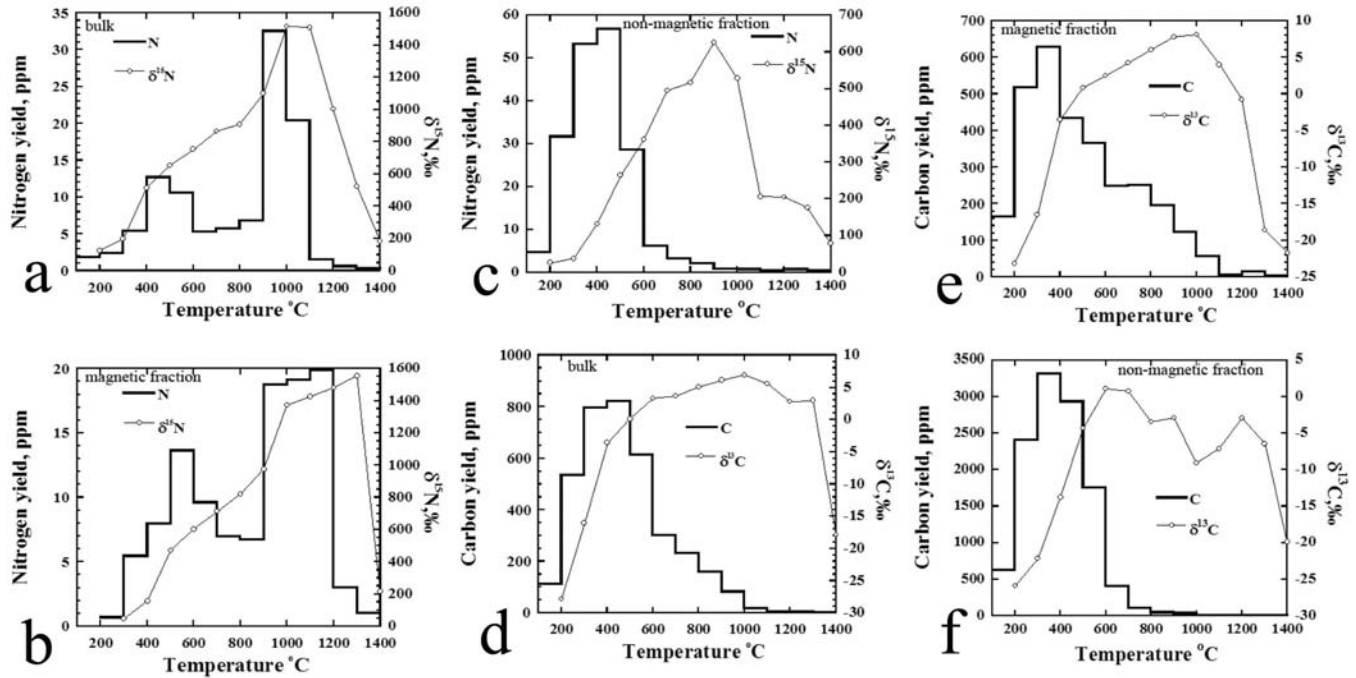


Fig. 18. Nitrogen (a–c) and carbon (d–f) release patterns and isotopic composition of bulk (a, d), magnetic fraction (b, e), and non-magnetic fraction (c, f) of Isheyev.

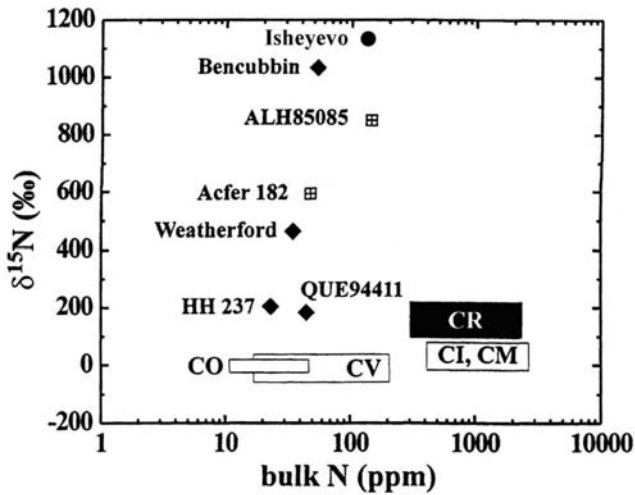


Fig. 19. Bulk nitrogen isotopic compositions of Isheyev. Compositional fields of other chondrite groups are from Weisberg et al. (1995) and Krot et al. (2003).

certainly influenced Isheyev. The mosaic extinction, planar fractures and planar deformation features of olivine grains indicate that Isheyev experienced shock metamorphism of shock stage S4. In contrast to other CH and CB<sub>b</sub> chondrites, most Fe,Ni-metal grains in Isheyev experienced thermal decomposition, suggesting the highest degree of thermal processing among metal-rich carbonaceous chondrites, which could be a result of shock metamorphism, parent body metamorphism due to decay heat of short-lived radio nuclides (Trieloff et al. 2003b), or hot accretion of components formed by a giant impact between planetary-size bodies (Krot et al.

2005). Since the disturbances by <sup>39</sup>Ar recoil and the possible presence of trapped Ar complicate the <sup>40</sup>Ar-<sup>39</sup>Ar age spectrum, we presently cannot distinguish whether secondary <sup>40</sup>Ar loss occurred during a late giant impact a few Ma after formation of the Isheyev parent body (Krot et al. 2005), or as late as <3.5 Ga ago, similar to <sup>40</sup>Ar-<sup>39</sup>Ar ages obtained for the glass of the Bencubbin meteorite (3.7–4.0 Ga; Kelly and Turner 1987).

The concentration of total trapped <sup>36</sup>Ar of Isheyev determined from our <sup>40</sup>Ar-<sup>39</sup>Ar study is  $19.6 \times 10^{-8} \text{ cm}^3 \text{ STP/g}$ , slightly less than that in CH chondrites (Table 6). In the first temperature extraction(s), it could be a terrestrial atmospheric component. Above 800 °C, radiogenic argon (<sup>40</sup>Ar\*) is very low and the <sup>40</sup>Ar\*/<sup>36</sup>Ar<sub>trapped</sub> ratios are rather low, between 3.4 and 4.5 for 7 extractions (Fig. 21). Trapped argon in these extractions is related to primordial and/or solar gases that are present in Isheyev (Nakashima et al. 2006) and possibly associated with Ca-bearing phases (judged from the concomitant release of neutron-induced <sup>37</sup>Ar from Ca), or metal phases (judged from the specific release temperature). It is an important question if the solar wind implanted gases were acquired during a very early epoch after dissipation of the solar nebula, e.g., during the chondrule producing giant impact advocated by Krot et al. (2005) or later in a typical asteroidal regolith setting. Our mineralogical observations indicate that Isheyev is not a “classic” breccia. This meteorite contains lithologies that differ in the proportion of metal and chondrules, and it does not contain fine-grained matrix at all, although it contains clasts of matrix material. Our preferred interpretation is that this texture is due to accretion of these

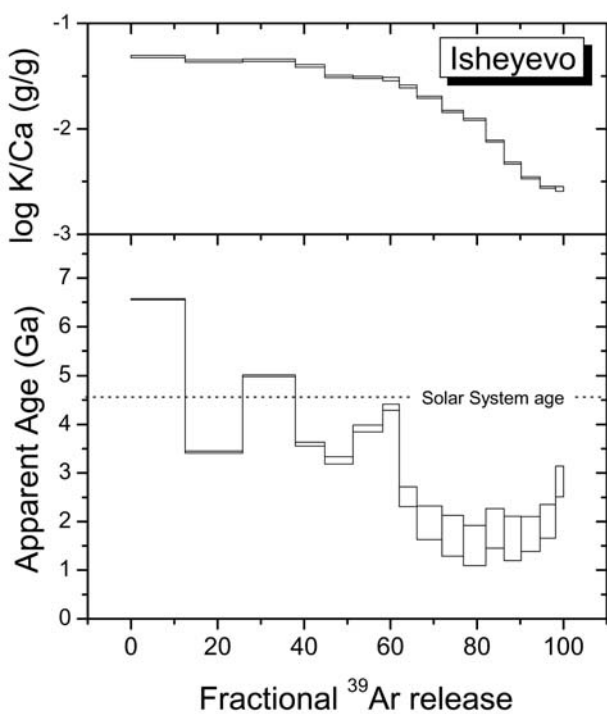


Fig. 20. K/Ca and age spectra of Isheyev. Ar-Ar age information is complicated by the  $^{39}\text{Ar}$  recoil effect and the possible presence of atmospheric trapped Ar at low temperatures. The total K-Ar age is  $4.27 \pm 0.02$  Ga. The bulk K and Ca contents from  $^{40}\text{Ar}/^{39}\text{Ar}$  data are  $87 \pm 4$  ppm and  $0.64 \pm 0.03\%$ , respectively.

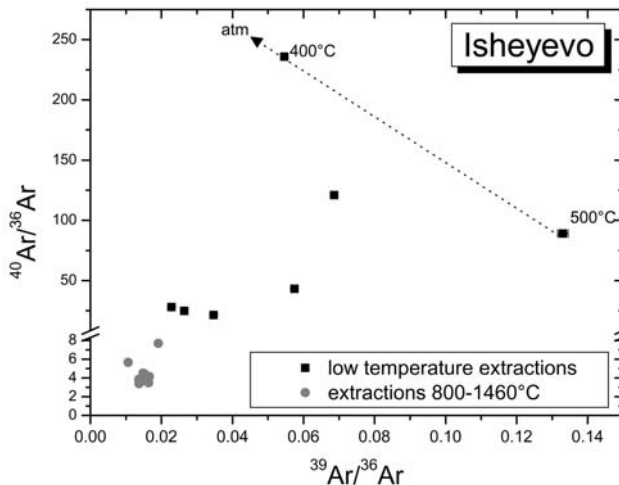


Fig. 21. Isochron plot of  $^{40}\text{Ar}/^{36}\text{Ar}$  versus  $^{39}\text{Ar}/^{36}\text{Ar}$  for Isheyev. First two temperature extractions probably contain trapped atmospheric argon. The trapped argon of high temperature extractions is of extraterrestrial origin.

components in the early solar nebula, which would favor a rather early implantation of solar wind noble gases.

The final stage preceding the meteorite's fall onto Earth is constrained by cosmogenic argon produced during exposure to galactic cosmic rays as meter-sized meteoroid. The calculated CRE age of 34 Ma (Table 6) is consistent with

that of the Bencubbin CB chondrite (Kelly and Turner 1987) of  $39 \pm 3$  Ma, while other CH chondrites have rather young CREs (HaH 237 [CB<sub>b</sub>] 3 Ma; PAT 91546 [CH] >8 Ma; PCA 92468 [CH] 4.3 Ma; RKP 02435 [CH] 1.5 Ma; Weber et al. 2001). Although these data are consistent that Bencubbin and Isheyev could be derived from the same parent body by the same excavation event, this certainly cannot be considered as compelling evidence.

## CONCLUSIONS

Isheyev is a metal-rich CH/CB<sub>b</sub>-like carbonaceous chondrite. It contains several lithologies with different abundances of Fe,Ni metal (7–90 vol%), and with different proportions of the similar components that, however, differ in sizes and relative proportions of porphyritic versus non-porphyritic chondrules. Fe,Ni-metal lithologies are dominant. The metal-poor lithology is texturally and mineralogically most similar to CH chondrites; the metal-rich lithologies are most similar to CB<sub>b</sub> chondrites.

Isheyev contains at least two populations of chondrules—mostly porphyritic chondrules (ferromagnesian, Al-rich, silica-rich, and Fe,Ni metal-rich), and metal-free, magnesian, cryptocrystalline, and skeletal olivine/pyroxene chondrules. These chondrules probably formed by different mechanisms: 1) melting of solid precursors, including chondrules of earlier generations and refractory inclusions, and 2) melting, evaporation, and condensation of solids during large-scale collision between planetary-size bodies.

Based on the textures and mineralogy, two populations of CAIs are identified: 1) very refractory, compact spherules composed of hibonite, grossite, Al-rich pyroxene, perovskite, gehlenitic melilite, and spinel, and 2) less refractory, igneous and non-igneous inclusions composed of melilite, Al,Ti-diopside, anorthite, and ±forsterite.

Several ferromagnesian layered chondrules experienced incipient aqueous alteration prior to incorporation into the Isheyev parent body. Although Isheyev contains abundant heavily hydrated lithic clasts, mineralogical observations excludes aqueous alteration of layered chondrules and lithic clasts in the same environment. We suggest that chondrules were hydrated by interaction with highly oxidized nebular gas, whereas lithic clasts experienced aqueous alteration in an asteroidal setting.

Bulk chemical and oxygen isotopic compositions of Isheyev are in the range of CH and CB chondrites. Bulk nitrogen isotopic composition is highly enriched in  $^{15}\text{N}$ . The magnetic fraction is very similar to the bulk sample in terms of both nitrogen release pattern and isotope profile; carbon released at high temperatures shows a relatively heavy isotope signature also.

We infer that Isheyev is a complex mixture of materials formed by different processes and under different physico-chemical conditions. All its constituents accreted together into the Isheyev parent asteroid in a region depleted in fine-

grained dust. This could have been a region in the early solar nebula in which the dusty and gaseous disk was already dissipated. Such a scenario is consistent with the presence of solar wind implanted noble gases in Isheyev, and with the comparatively old K-Ar age. On the other hand, we cannot exclude that the K-Ar system was affected by a later collisional event.

The cosmic-ray exposure age of Isheyev determined by cosmogenic  $^{38}\text{Ar}$  is ~34 Ma similar to that of the Bencubbin meteorite.

**Acknowledgments**—We thank L. D. Barsukova, I. A. Roshchina, and A. L. Lorenz for their assistance in determination of bulk chemical composition of Isheyev by XRF and INAA analyses. Also we thank V. K. Karandashev (Institute of Microelectronics and Extra-Pure Materials Technologies of Russian Academy of Sciences) for his assistance in determination of bulk compositions by ICP-MS analysis. We thank Buikin A. I. for his assistance in  $^{40}\text{Ar}$ - $^{39}\text{Ar}$  dating. We also thank J. Zipfel, R. H. Jones, M. K. Weisberg, A. Meibom, and D. Hezel for their fruitful reviewers and discussion, which led to improvement of the paper. This work was supported by grant RFBR-BSTS (project N14/04 and 03-05-20008), Austrian Academy of Sciences (FWF, Austria), PPARC, UK, Deutsche Forschungsgemeinschaft (DFG) and Forschungszentrum Geesthacht (GKSS), and NASA grant NAG5-10610 (A. N. Krot, P. I.).

**Editorial Handling**—Dr. Cyrena A. Goodrich

## REFERENCES

- Anders E. and Grevesse N. 1989. Abundances of the elements: Meteoritic and solar. *Geochimica et Cosmochimica Acta* 53:197–214.
- Bischoff A. and Keil K. 1984. Al-rich objects in ordinary chondrites—Related origin of carbonaceous and ordinary chondrites and their constituents. *Geochimica et Cosmochimica Acta* 48:693–709.
- Bischoff A., Palme H., Ash R. D., Clayton R. N., Schultz L., Herpers U., Stöffler D., Grady M. M., Pillinger C. T., Spettel B., Weber H., Grund T., Endreb M., and Weber D. 1993a. Paired Renazzo-type (CR) carbonaceous chondrites from the Sahara. *Geochimica et Cosmochimica Acta* 57:1587–1604.
- Bischoff A., Palme H., Schultz L., Weber D., Weber H. W., and Spettel B. 1993b. Acfer 182 and paired samples, an iron-rich carbonaceous chondrite: Similarities with ALH 85085 and relationship to CR chondrites. *Geochimica et Cosmochimica Acta* 57:2631–2648.
- Brereton N. R. 1970. Corrections for interfering isotopes in the  $^{40}\text{Ar}$ - $^{39}\text{Ar}$  dating method. *Earth and Planetary Science Letters* 8:427–433.
- Campbell A. J., Humayun M., Meibom A., Krot A. N., and Keil K. 2001. Origin of layered metal in the QUE 94411 chondrite. *Geochimica et Cosmochimica Acta* 65:163–180.
- Campbell A. J., Humayun M., and Weisberg M. K. 2002. Siderophile element constraints on the formation of metal in the metal-rich chondrites Bencubbin, Weatherford, and Gujba. *Geochimica et Cosmochimica Acta* 66:647–660.
- Campbell A. J. and Humayun M. 2004. Formation of metal in the CH chondrites ALH 85085 and PCA 91467. *Geochimica et Cosmochimica Acta* 68:3409–3422.
- Ciesla F. J., Lauretta D. S., Cohen B. A., and Hood L. L. 2003. A nebular origin for chondritic fine-grained phyllosilicates. *Science* 299:549–552.
- Clayton R. N. and Mayeda T. K. 1999. Oxygen isotope studies of carbonaceous chondrites. *Geochimica et Cosmochimica Acta* 63: 2089–2104.
- Ebel D. S. and Grossman L. 2000. Condensation in dust-enriched systems. *Geochimica et Cosmochimica Acta* 64:339–366.
- Eugster O. 1988. Cosmic-ray production rates for  $^3\text{He}$ ,  $^{21}\text{Ne}$ ,  $^{38}\text{Ar}$ ,  $^{83}\text{Kr}$ , and  $^{126}\text{Xe}$  in chondrites based on  $^{81}\text{Kr}/\text{Kr}$  exposure ages. *Geochimica et Cosmochimica Acta* 52:1649–1662.
- Franchi I. A., Wright I. P., and Pillinger C. T. 1986. Heavy nitrogen in Bencubbin—A light element isotopic anomaly in a stony iron meteorite. *Meteoritics & Planetary Science* 36:401–418.
- Franchi I. A., Sexton A. S., and Pillinger C. T. 1998. Oxygen isotope variation in the Bencubbin meteorite: An exotic component in the matrix (abstract)? *Meteoritics & Planetary Science* 33:A53.
- Grady M. M. and Pillinger C. T. 1990. ALH 85085—Nitrogen isotope analysis of a highly unusual primitive chondrite. *Earth and Planetary Science Letter* 97:29–40.
- Greshake A., Krot A. N., Meibom A., Weisberg M. K., and Keil K. 2002. Heavily hydrated matrix lumps in the CH and metal-rich chondrites QUE 94411 and Hammadah al Hamra 237. *Meteoritics & Planetary Science* 37:281–294.
- Grossman J. N., Rubin A. E., and MacPherson G. J. 1988. ALH 85085: A unique volatile-poor carbonaceous chondrite with possible implications for nebular fractionation processes. *Earth and Planetary Science Letters* 91:33–54.
- Grossman J. N. and Zipfel J. 2001. The Meteoritical Bulletin, No. 85, 2001 September. *Meteoritics & Planetary Science* 36:A293–322.
- Gounelle M., Young E. D., Shahar A., Tonui E., and Kearsley A. 2007. Magnesium isotopic constraints on the origin of CB<sub>b</sub> chondrites. *Earth and Planetary Science Letters* 256:521–533.
- Hezel D. C., Brenker F. E., and Palme H. 2002. Petrology and cooling history of cryptocrystalline chondrules from CH chondrites (abstract #1787). 33rd Lunar and Planetary Science Conference. CD-ROM.
- Hezel D. C., Palme H., Brenker F. E., and Nasdala L. 2003. Evidence for fractional condensation and reprocessing at high temperatures in CH chondrites. *Meteoritics & Planetary Science* 38:1199–1215.
- Ivanova M. A., Petaev M. I., Nazarov M. A., Taylor L. A., MacPherson G. J., and Wood J. A. 2001. A record of nebular processes in different constituents of the CH chondrite NWA 470 (abstract). *Meteoritics & Planetary Science* 36:A88.
- Ivanova M. A., Kononkova N. N., Franchi I. A., Verchovsky A. B., Korochantseva E. V., Trieloff M., Krot A. N., and Brandstätter F. 2006. Isheyev meteorite: Genetic link between CH and CB chondrites (abstract #1100)? 37th Lunar and Planetary Science Conference. CD-ROM.
- Jessberger E. K., Dominik B., Staudacher Th., and Herzog G. F. 1980.  $^{40}\text{Ar}$ - $^{39}\text{Ar}$  ages of Allende. *Icarus* 42:380–405.
- Jones R. H., Grossman J. N., and Rubin A. E. 2005. Chemical, mineralogical, and isotopic properties of chondrules: Clue to their origin. In *Chondrites and the protoplanetary disk*, edited by Krot A. N., Scott E. R. D., Reipurth B. San Francisco: The Astronomical Society of the Pacific. pp. 251–286.
- Kelly S. and Turner G. 1987. Laser probe  $^{40}\text{Ar}$ - $^{39}\text{Ar}$  investigation of the polymict breccia Bencubbin. *Meteoritics* 22:427.
- Korochantseva E. V., Trieloff M., Lorenz C. A., Buykin A. I., Ivanova M. A., Schwarz W. H., Hopp J., and Jessberger E. K. 2007. L-chondrite asteroid breakup tried to Ordovician meteorite

- shower by multiple isochron  $^{40}\text{Ar}$ - $^{39}\text{Ar}$  dating. *Meteoritics & Planetary Science* 42:113–130.
- Krot A. N., Meibom A., Petaev M. I., Keil K., Zolensky M. E., Saito A., Mukai M., and Ohsumi K. 2000. Ferrous silicate spherules with euhedral iron-nickel metal grains from CH carbonaceous chondrites: Evidence for supercooling and condensation under oxidizing conditions. *Meteoritics & Planetary Science* 35:1249–1258.
- Krot A. N., Meibom A., Russel S. S., Alexander C. M. O'D., Jeffries T. E., and Keil K. 2001a. A new astrophysical setting for chondrule formation. *Science* 291:1776–1779.
- Krot A. N., McKeegan K. D., Russel S. S., Meibom A., Weisberg M. K., Zipfel J., Krot T. V., Fagan T. J., and Keil K. 2001b. Refractory Ca,Al-rich inclusions and Al-diopside-rich chondrules in the metal-rich chondrites Hammadah al Hamra 237 and QUE 94411. *Meteoritics & Planetary Science* 36:1189–1217.
- Krot A. N. and Keil K. 2002. Anorthite-rich chondrules in CR and CH carbonaceous chondrites: Genetic link between Ca, Al-rich inclusions and ferromagnesian chondrules. *Meteoritics & Planetary Science* 37:91–111.
- Krot A. N., Meibom A., Weisberg M. K., and Keil K. 2002a. The CR chondrite clan: Implications for early solar system processes. *Meteoritics & Planetary Science* 37:1451–1490.
- Krot A. N., Hutcheon I. D., and Keil K. 2002b. Anorthite-rich chondrules in the reduced CV chondrites: Evidence for complex formation history and genetic links between CAIs and ferromagnesian chondrules. *Meteoritics & Planetary Science* 37:155–182.
- Krot A. N., Amelin Y., Cassen P., and Meibom A. 2005. Young chondrules in CN chondrites from a giant impact in the early solar system. *Nature* 436:989–992.
- Krot A. N., Ulyanov A. A., Ivanova M. A., and Russel S. S. 2006a. Origin of chondrules in the metal-rich carbonaceous chondrites (abstract #1224). 37th Lunar and Planetary Science Conference. CD-ROM.
- Krot A. N., Ivanova M. A., and Ulyanov A. A. 2006b. Chondrules in the CB/CH-like carbonaceous chondrite Isheyevo: Evidence for various chondrule-forming mechanisms and multiple chondrule generations. *Chemie der Erde* 67:283–300.
- Krot A. N., Ulyanov A. A., and Ivanova M. A. Forthcoming. Refractory inclusions in the CB/CH-like carbonaceous chondrite Isheyevo: I. Mineralogy and petrography. *Meteoritics & Planetary Science* 43.
- Krot A. N., Nagashima K., Huss G. R., Bizzarro M., Ciesla F. J., and Ulyanov A. A. 2007a. Relict refractory inclusions in magnesium porphyritic chondrules from the CH and CH/CB carbonaceous chondrites (abstract). *Meteoritics & Planetary Science* 42:A90.
- Krot A. N., Nagashima K., and Ulyanov A. A. 2007b. Oxygen isotopic compositions of calcium-aluminum-rich inclusions and chondrules in the CB/CH-like carbonaceous chondrite Isheyevo. (abstract #1888). 38th Lunar and Planetary Science Conference. CD-ROM.
- Krot A. N., Nagashima K., Bizzarro M., Huss G. R., Davis A. M., McKeegan K. D., Meyer B. S., and Ulyanov A. A. 2007c. Multiple generations of refractory inclusions in the metal-rich carbonaceous chondrites Acfer 182/214 and Isheyevo. *The Astrophysical Journal* 672:713–721.
- McSween H. Y. Jr. and Richardson S. M. 1977. The composition of carbonaceous chondrite matrix. *Geochimica et Cosmochimica Acta* 41:1145–1161.
- Meibom A., Petaev M. I., Krot A. N., Wood J. A., and Keil K. 1999. Primitive Fe,Ni metal grains in CH carbonaceous chondrites formed by condensation from a gas of solar composition. *Journal of Geophysical Research* 104:22,053–22,059.
- Meibom A., Desch S. J., Krot A. N., Cuzzi J. N., Petaev M. I., Wilson L., and Keil K. 2000. Large-scale thermal events in the solar nebula: Evidence from Fe,Ni metal grains in primitive meteorites. *Science* 288:839–841.
- Meibom A., Petaev M. I., Krot A. N., Keil K., and Wood J. A. 2001. *Journal of Geophysical Research* 106:32,797–32,801.
- Meibom A., Righter K., Chabot N., Dehn G., Antignano A., McCoy T. J., Krot A. N., Zolensky M. E., Petaev M. I., and Keil K. 2005. Shock melts in QUE 94411, Hammadah al Hamra 237, and Bencubbin: Remains of the missing matrix? *Meteoritics & Planetary Science* 40:1377–1391.
- Miller M. F., Franchi I. A., and Pillinger C. T. 1999. High-precision measurements of the oxygen isotope mass-dependent fractionation line for the Earth-Moon system (abstract #1729). 30th Lunar and Planetary Science Conference. CD-ROM.
- Nakashima D., Schwenzer S. P., Franke L., Ott U., Ivanova M. A., Buikin A. I., Trieloff M., Korochantseva E. V., and Hopp J. 2006. Noble gases in the Isheyevo meteorite (abstract). *Meteoritics & Planetary Science* 41:A129.
- Petaev M. I., Meibom A., Krot A. N., Wood J. A., and Keil K. 2001. The condensation origin of layered metal grains in QUE 94411: Implications for the formation of the Bencubbin-like chondrites. *Meteoritics & Planetary Science* 36:93–106.
- Rooke G. P., Franchi I. A., Verchovsky A. B., and Pillinger C. T. 1998. The relationship between noble gases and the heavy nitrogen in polymict ureilites (abstract #1744). 29th Lunar and Planetary Science Conference. CD-ROM.
- Rubin A. E., Kallemeyn G. W., Wasson J. T., Clayton R. N., Mayeda T. K., Grady M., Verchovsky A. B., Eugster O., and Lorenzetti S. 2003. Formation of metal and silicate globules in Gujba: A new Bencubbin-like meteorite fall. *Geochimica et Cosmochimica Acta* 67:3283–3298.
- Russel S., Zipfel J., Grossman J. N., and Grady M. M. 2002. The Meteoritical Bulletin, No. 86, 2002 July. *Meteoritics & Planetary Science* 37:A157–A184.
- Schäffer G. A. and Schäffer O. A. 1977.  $^{40}\text{Ar}$ - $^{39}\text{Ar}$  ages of lunar rocks. Proceedings, 8th Lunar Science Conference. pp. 2253–2300.
- Schultz L., Weber H. W., and Begemann F. 1991. Noble gases in H chondrites and potential differences between Antarctic and non-Antarctic meteorites. *Geochimica et Cosmochimica Acta* 55:59–66.
- Scott E. R. D. 1988. A new kind of primitive chondrite, Allan Hills 85085. *Earth and Planetary Science Letters* 91:1–18.
- Steiger R. H. and Jäger E. 1977. Subcommission on geochronology: Convention on the use of decay constants in geo- and cosmochronology. *Earth and Planetary Science Letters* 36:359–362.
- Stöffler D., Keil K., and Scott E. R. D. 1991. Shock metamorphism of ordinary chondrites. *Geochimica et Cosmochimica Acta* 55: 3845–3867.
- Sugiura N., Zashu S., Weisberg M. K., and Prinz M. 1999. H, C, and N isotopic compositions of bencubbinites (abstract #1329). 30th Lunar and Planetary Science Conference. CD-ROM.
- Sugiura N., Zashu S., Weisberg M. K., and Prinz M. 2000. A nitrogen isotope study of bencubbinites. *Meteoritics & Planetary Science* 36:401–418.
- Trieloff M., Deutsch A., and Jessberger E. K. 1998. The age of the Kara impact structure, Russia. *Meteoritics & Planetary Science* 33:361–372.
- Trieloff M., Falter M., and Jessberger E. K. 2003a. The distribution of mantle and atmospheric argon in oceanic basalt glasses. *Geochimica et Cosmochimica Acta* 67:1229–1245.
- Trieloff M., Jessberger E. K., Herrwerth I., Hopp J., Fieni C., Ghelis M., Bourot-Denise M., and Pellat P. 2003b. Structure and thermal history of the H-chondrite parent asteroid revealed by thermochronometry. *Nature* 422:502–506.
- Trieloff M., Falter M., Buikin A. I., Korochantseva E. V., Jessberger

- E. K., and Altherr R. 2005. Argon isotope fractionation induced by stepwise heating. *Geochimica et Cosmochimica Acta* 69: 1253–1264.
- Turner G. 1971.  $^{40}\text{Ar}$ - $^{39}\text{Ar}$  dating: The optimization of irradiation parameters. *Earth and Planetary Science Letters* 10:227–234.
- Turner G., Enright M. C., and Cadogan P. H. 1978. The early history of chondrite parent bodies inferred from  $^{40}\text{Ar}$ - $^{39}\text{Ar}$  ages. Proceedings, 9th Lunar Science Conference. pp. 989–1025.
- Verchovsky A. B., Fisenko A. V., Semenova L. F., and Pillinger C. T. 1988. Heterogeneous distribution of xenon-HL within presolar diamonds (abstract). *Meteoritics & Planetary Science* 32:A131–132.
- Wasson J. T. and Kallemeyn G. W. 1990. Allan Hills 85085: A subchondritic meteorite of mixed nebular and regolith heritage. *Earth and Planetary Science Letters* 101:148–161.
- Weber H. W., Franke L., and Schultz L. 2001. Subsolar noble gases in metal-rich carbonaceous (CH) chondrites. *Meteoritics & Planetary Science* 36:A220.
- Weisberg M. K., Prinz M., and Nehru C. E. 1988. Petrology of ALH 85085: A chondrite with unique characteristics. *Earth and Planetary Science Letters* 91:19–32.
- Weisberg M. K., Prinz M., Clayton R. N., Mayeda T. K., Grady M. M., and Pillinger C. T. 1995. The CR chondrite clan. *Proceedings of the NIPR Symposium on Antarctic Meteorites* 8: 11–32.
- Weisberg M. K., Prinz M., Clayton R. N., Mayeda T. K., Sugiura N., Zashu S., and Ebihara M. 2001. A new metal-rich chondrite grouplet. *Meteoritics & Planetary Science* 36:401–418.
- Weisberg M. K., Connolly H. C. Jr., and Ebel D. S. 2004. Petrology and origin of amoeboid olivine aggregates in CR chondrites. *Meteoritics & Planetary Science* 39:1741–1753.
- Wright I. P., Boyd S. R., Franchi I. A., and Pillinger C. T. 1988. High-precision determination of nitrogen stable isotope ratios at the sub-nanomole level. *Journal of Physics E* 21:865–875.
- Wright I. P. and Pillinger C. T. 1989. Carbon isotopic analysis of small samples by use of stepped-heating extraction and static mass spectrometry. *U.S. Geological Bulletin* 7890:9–34.
- Zipfel J., Wlotzka F., and Spettel B. 1998. Bulk chemistry and mineralogy of a new “unique” metal-rich chondritic breccia, Hammadah al Hamra 237 (abstract #1417). 29th Lunar and Planetary Science Conference. CD-ROM.